2010 DWH Offshore Water Column Samples—Forensic Assessments and Oil Exposures

Contents

James R. Payne, Ph.D.
Payne Environmental Consultants, Inc.
1991 Village Parkway, Suite 206B
Encinitas, CA 92024
760-613-7391 (cell)
jrpayne@sbcglobal.net

William B. Driskell
6536 20th Ave NE
Seattle, WA 98115
206-522-5930
bdriskell@comcast.net

Table of Figures

List of Tables

List of Acronyms

AQAP	Analytical Quality Assurance Plan produced by EcoChem data validators
BTEX	Benzene, Toluene, Ethylbenzene, Xylenes (o and m/p); volatile aromatics of primary interest
CDOM	Colored dissolved organic material or fluorometry instrument designed to measure waterborne CDOM
CTD	Combined conductivity, temperature, and depth measuring instrument
D/P ratios	Forensic diagnostic, dibenzothiophene/phenanthrene ratios
DO	Dissolved oxygen
DOR	Dispersant to oil ratio, dispersant application rate
DOSS	Dioctyl-sulfosuccinate, active surfactant ingredient in Corexit dispersants

DWHOS	Deepwater Horizon Oil Spill
FBOB FTOB	Water sampling bias incurred from sampling From Bottom (or Top) of collection Bottle
FID	Flame ionization detector, used in conjunction with GC to measure SHC
FT ICR	Forrier-transform Ion cyclotron resonance
GC/MS	Gas chromatograph/Mass spectrometer, instrument used to separate oil analytes and detect their abundance
GE	Glycol ethers, alt. di(propylene glycol)-n-butyl ether (DPNB)
Holocam	Holographic camera used for particulate-oil droplet-size measurements
LCMS	Liquid chromatography/mass spectrometer, similar to GC/MS but using LC methods to separate analytes
LISST	Laser in-situ Scattering and Transmissometry instrument
OSAT	Operational Scientific Advisory Team
PAH	Polycyclic aromatic hydrocarbons
PIANO	Paraffins, isoparaffins, aromatics, napthenes, and olefins; method for measuring VOC and other analytes.
PLVWSS	Portable large volume water sampling system; field filtering system for separating dissolved and particulate fractions of water samples
ROV	Remotely operated vehicles; used eventually as combined observation, instrumentation and sample-collection platforms.
RPS ASA	Applied Science Associates consultants
SHC	Saturated hydrocarbons or aliphatics, also AHC, alkanes or TPH
SIM	Selected ion monitoring mode; instrument/method used for measuring PAH and biomarkers
SIMAP	Spill Impact Model Application Package, RPS Applied Science Associates
SMART	Dispersant-application monitoring protocols
TPAH50	Sum of 50 selected PAH (naphthalene to benzo(GHI)perylene less retene and perylene)
TPAH42	Petrogenic portion of TPAH50 (less 6-ringed pyrogenic PAH)
UV	Ultraviolet light
VOC	Volatile organic compounds (alt. VOA for analyses)

DRAFT
2010 DWH Offshore Water Column Samples—Forensic Assessments and Oil Exposures

James R. Payne, Ph.D. and William B. Driskell August 2015

Executive Summary

The objective of this study was to assess the presence of MC252 oil in offshore water samples collected under NRDA protocols in 2010. In the field, water containing oil was collected with grab samplers in addition to being observed, photographed, and tracked in conductivity, temperature, and depth (CTD), dissolved oxygen (DO), and fluorometry profiles. Forensic evaluations of analytic data, field instruments, and observations lead to the following findings:

- Hydrocarbon chemistry and corroborating field data positively link MC252 oil to offshore oil in near-surface waters, rising through the water column near the wellhead (cone of gas and oil droplets), and entrained in an extensive deepwater oil plume (1,000-1,400m trap depth) advecting predominantly to the Southwest with occasional shallower lenses.
- The deepwater plume has been tracked 412 km SW of the wellhead as positive matches confirmed by corroborating lines of evidence (i.e., depth, fluorometry spikes, DO sags, and dispersant indicators) and out to 267 km as detailed, phase-discriminated, positive matches.
- With increasing time and distance from the wellhead, the deepwater plume PAH signal became diluted and no longer detectible using standard GC/MS methods whereupon reliance on corroborating data (depth, fluorometry signals, DO sags, and persistent dispersant constituents) became more important in tracking the deepwater plume. We hypothesize that the absence of detectable PAH or other hydrocarbons in samples exhibiting corroborating evidence for oil's presence may be, at least in part, attributable to the presence of oxygenated and polar microbial degradation products not detectible using standard GC/MS methods.
- Effects of dispersant treatments, both as surface applications and injected at the wellhead, were seen in the oil profiles as enhanced weathering patterns and increased dissolution, thus implying dispersants were an effective mediation treatment (dispersants are discussed in a separate report).
- Generally, near-surface oil samples showed evidence of substantial dissolution weathering as the oil droplets rose through the water column, as well as enhanced evaporative losses of lower-molecular-weight n-alkanes and aromatic hydrocarbons. Oil that had reached the surface also showed evidence of photo-oxidation of alkylated chrysenes.
- Typical of surface oil dynamics, near-surface increases in dissolved and particulate-oil fractions were observed as a result of wind-induced entrainment of surface films and dispersant effects.

Note that four other documents produced by the authors also relate to offshore water samples: 1) Forensic Fingerprinting Methods (Payne and Driskell, 2015a); 2) Dispersant Effects (Payne and Driskell, 2015b); and 3) Offshore Adaptive Sampling Strategies (Payne and Driskell, 2015c).

Introduction

Early in the response to the Deepwater Horizon (DWH) blowout, remotely-operated-vehicle (ROV) operators monitoring the wellhead reported encountering oil layers, primarily at ~1,000 m depth (pers comm, *Skansi Neptune*, 2010). Later OSAT, academic, and NRDA sampling confirmed these

observations, finding polycyclic aromatic hydrocarbon (PAH) constituents, dispersant indicators, and selected BTEX (benzene, toluene, ethylbenzene, and xylenes) in the 900-1,400m depth range (Figure 1 and Figure 2). While the chemical character of this layer was not a complete surprise, understanding the formation of the deep plume required further observations and insights (Socolofsky et al., 2011; also chronicled in Payne and Driskell, 2015c).

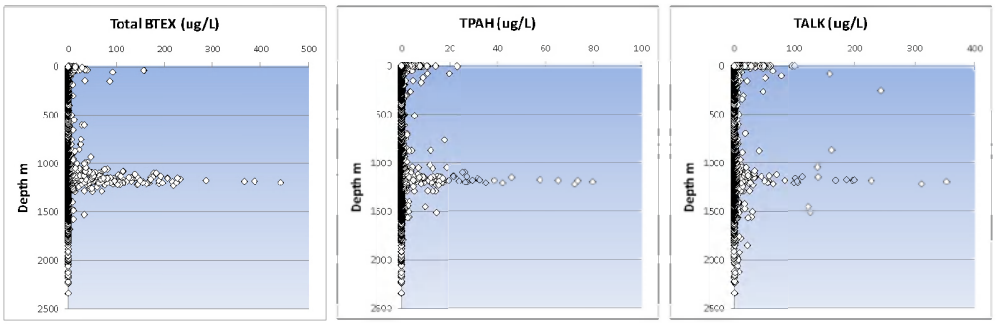

Figure 1. Depth distribution of total BTEX, total PAH (TPAH) and total alkanes (TALK) measured in seawater collected throughout the Gulf of Mexico between 11 May and 15 December 2010. [Data source: public Operational Science Advisory Team (OSAT) and GeoPlatform.gov data.]

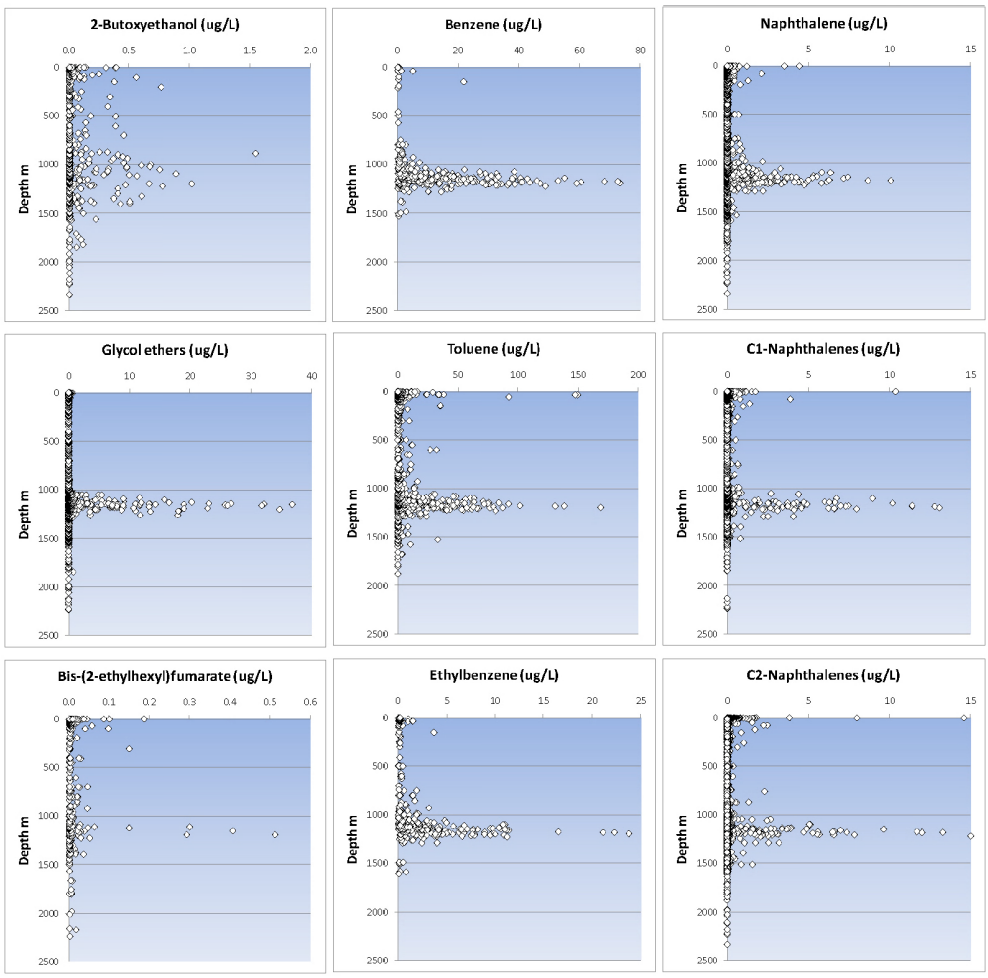

Figure 2. Depth distribution of three dispersant indicators, 2-butoxyethanol, glycol ethers, and bis-(2-ethylhexyl) fumerate, and selected BTEX and PAH constituents measured in seawater collected throughout the Gulf of Mexico between 11 May and 15 December 2010. [Data source: public Operational Science Advisory Team (OSAT) and GeoPlatform.gov data.]

Briefly, when oil is released into seawater, its hydrocarbon components partition into dissolved and particulate (oil-droplet) phases (Payne et al., 1984, 1991a, b; Payne and McNabb, Jr. 1984; NRC 1985, 1989, 2003, 2005; Wolfe et al., 1994; Payne and Driskell, 2003; Reddy et al., 2011; Camilli et al., 2011). Volatile aromatics such as BTEX and other alkylated benzenes along with lower-molecular-weight PAH all appreciably dissolve in seawater in a generally predictable manner (NRC 2003, 2005). During the Macondo blowout, however, the partitioning activities were quite dynamic. Oil droplets and gas bubbles separated in the well's multiphasic, jetted flow resulted in an almost complete dissolution of lower-molecular-weight aliphatics (at least through heptane, McAuliffe, 1987) and aromatics (alkylated benzenes) (Reddy et al., 2011), and a more limited dissolution of C8-C13 aliphatics and two- and three-ring aromatics (alkylated naphthalenes, fluorenes, phenanthrenes/anthracenes, and dibenzothiophenes). Similar behavior was observed during the IXTOC I blowout in the Bay of Campeche, GOM in 1979 (Payne et al., 1980a, b; Boehm and Fiest, 1982). During the DWH event, Ryerson et al. (2011) also

confirmed selective removal of BTEX and the lighter PAH in the airborne evaporated hydrocarbons captured above the DWH blowout.

Oil partitioning processes have been reviewed in detail in several National Research Council reports (2003, 2005), and more recently by Faksness (2007). However, despite this knowledge, there have been only a few efforts to collect phase-discriminated data in actual oil-spill-related Natural Resource Damage Assessments (NRDA). In 1999, portable field-filtration equipment was built for this task (Payne et al., 1999). In addition to obtaining individually quantified dissolved- and particulate-oil phase data, filtering larger sample volumes at the time of collection (3.5 L versus typically sending 1 L whole-water samples to the lab) provides more of an oil signal and thus, improves method detection limits. These more detailed and precise data improve forensic assessment, insights of oil fate and transport processes, and provide dissolved phase estimates for more accurate toxicological assessments.

First utilized in response to the *New Carissa* oil spill (Coos Bay, Oregon, 1999), this approach was highly successful in discriminating the phase signatures with low ppb resolution (Payne and Driskell, 2001). The resulting data validated spatial model predictions of oil fate, transport, and impacts, specifically demonstrating that while the dissolved-phase signal appeared in crab tissue and interstitial water on an otherwise visibly unoiled beach, the associated micro-droplet phase appeared in tissues of nearby filter-feeding mussels and oysters (Payne and Driskell, 2001, 2003). Later, in Port Valdez, Alaska, Payne et al. (2005) used this same approach to assess phase signatures in subsurface effluents discharged from the Ballast Water Treatment Facility at the Alyeska Marine Terminal, tracking the phase signatures to a seasonal uptake in the port's mussels.

Assessing phase discrimination is even more pertinent for interpreting DWH water samples. In deep water, oil-weathering processes comprise phase partitioning (dissolution) and advection/diffusion of dissolved- and increasingly weathered, particulate-oil fractions until microbial or chemical oxidation, or sedimentation processes eventually degrade or remove the phase-separated hydrocarbons from the water column. The DWH was not a simple spill. With an unprecedented deep and lengthy release along with complex droplet-entrainment dynamics, a slow to-and-fro advection around and eventually away from the wellhead, and a unique, accelerated, dispersant-mediated dissolution behavior at depth, each of these factors will modify the oil signature as the released oil weathers.

For DWH resource injury assessments, rather than relying solely on exposure maps from the water chemistry sampling efforts, modeling was slated to be used as a tool to calculate impacts. Since the actual water-column sampling was neither synoptic nor sufficiently comprehensive to document hydrocarbon concentrations within the entire impact region, the forensic results were intended to be used to validate model estimates by providing representative water samples' phase-characterized composition.

Commensurate with the scale of the event, there are currently no less than twenty-nine different academic and agency papers describing the nature and potential toxicity of the deep plume in the published literature (Camilli, *et al.*, 2010, Diercks, 2010, Hazen, *et al.*, 2010, Boehm, et al., 2011; Camilli, *et al.*, 2011, Kujawinski, *et al.*, 2011, Mariano, *et al.*, 2011, McNutt, *et al.*, 2011, , Reddy, *et al.*, 2011, Redmond and Valentine, 2011, Socolofsky, *et al.*, 2011, Du and Kessler, 2012, Allan, et al., 2012; Lubchenco, *et al.*, 2012, McNutt, *et al.*, 2012, Passow, et al., 2012; Yapa, et al., 2012; Ryerson, *et al.*, 2012; Brandvik, et al., 2013; Hall et al., 2013; Incardona, et al., 2013; Johansen, et al., 2013; Prince et al., 2013; Spier et al., 2013; Crespo-Medina, et al., 2014; Gray, et al., 2014; Liu, et al., 2014; Smith, et al., 2014; White et al., 2014). Most of these authors, however, used very limited data sets. There are now over 15,000 samples with inclusion of additional, independent BP and Response cruise efforts and pre-impact near-shore water samples collected by local, state, and federal agency representatives. While only 5,332 cruise samples collected through December 2010 were considered for this document, and of those,

4,189 forensically characterized, these data alone confirm DWH BTEX and PAH distributions occurred on a vast spatial and temporal scale throughout the water column.

Methods

Field Methods

Sampling the Plumes

The primary sampling challenge for this event was in finding, tracking, and characterizing the entrapped deepwater oil plume that was first reported by wellhead ROV operators (detailed in Payne and Driskell, 2015c). While surface slicks were of interest, they were forming and transporting in a predictable fashion, tracked mostly by remote imaging, oceanographic models, and shoreline surveys. Other than initially documenting near-surface weathering and dissolution processes, slicks did not require the degree of effort necessary for tracking and sampling the deepwater plume and were thus, a smaller component in the offshore sampling (~18% of forensically reviewed samples came from the top 20 m).

Initially, water collection efforts were focused near the wellhead or within the basin of the blowout, but they began to move further afield as knowledge of the deep plume's behavior developed. Note that the time series of sampling efforts merely reflect this moving spatial focus, i.e., the samples were only exploratory snapshots that do not represent a comprehensive view of timing nor exposure. Again, the data are primarily intended to document exposure and characterize oil-fate processes, as well as verify model results.

Tracking the deepwater oil plume required innovative and adaptive efforts. Any oceanographic vessel, by design, can retrieve water samples from depth. But naively collecting random or systematic samples on a cast, as some cruises did, was unlikely to encounter the discrete deep plume. Only by using a combination of CTD, fluorescence, dissolved oxygen, and predictive modeling, plus on some cruises, ROV visuals (Payne and Driskell, 2015c), did field collections become successful and effective in finding and sampling the deepwater oil plume. The sensor data were also highly relevant in later corroborating forensic chemistry results (Payne and Driskell, 2015a).

As part of the DWH NRDA effort, over 11,126 discrete water samples (including QC) were collected from numerous vessels-of-opportunity near the wellhead during the initial weeks of the incident, starting in May 2010, and then further afield during the subsequent months through the fall of 2011. Water samples were collected mostly from conventional Go-Flo or Niskin bottles, preserved by refrigeration or acidification in the field after collection, and later shipped and held refrigerated at the lab. After an extensive logistical and laboratory-extraction effort, only 217 of 22,039 processed water samples (0.98%) were compromised by exceeding the 14-day maximum hold time specified by the project's Analytical Quality Assurance Plan (AQAP).

The previously mentioned, phase-partitioned samples were collected in 2010 on several cruise legs aboard the *Jack Fitz* and the *HOS Davis* and in 2011, the *HOS Sweet Water*. Whole-water samples were vacuumed through 0.7 µm glass-fiber filters at sea immediately upon collection using the Portable Large Volume Water Sampling System (PLVWSS) developed by Payne et al. (1999). After filtration, the filters containing the particulate/oil phase (commonly termed as "Payne filters") were frozen in Certified-Clean glass jars and shipped to Alpha Analytical Laboratories. The 3.5 L dissolved-phase samples were refrigerated in the original, Certified-Clean, 3.8 L (1 gal), amber-glass collection jugs from the PLVWSS and shipped to the laboratory for the same analyses.

Analytical Laboratory Methods

Nearly all of the NOAA-NRDA water-column samples were analyzed by Alpha Analytical Laboratory (Mansfield, Massachusetts) for detailed hydrocarbon composition in accordance with the AQAP. Analyte lists are detailed in the AQAP but briefly included:

- Total Extractable Hydrocarbons (TEH) and Saturated Hydrocarbon Compounds (SHC): a modified EPA Method 8015B was used to determine the total extractable petroleum hydrocarbons (TEH/SHC also commonly referred to as TPH) concentration (C_9-C_{44}) and concentrations of individual n-alkanes (C_9-C_{40}) and (C_{15}-C_{20}) acyclic isoprenoids (e.g., pristane and phytane), and simultaneously provide a high resolution gas chromatography-flame ionization detection (GC/FID) fingerprint of the samples. The concentrations of target aliphatic compounds presented herein are reported in µg/L (ppb) for both dissolved-phase and particulate/oil (filter) samples and are not surrogate-recovery corrected.
- PAH, Alkylated PAH, and Petroleum Biomarkers: semi-volatile compounds in each sample were analyzed using Selected Ion Monitoring (SIM) gas chromatography/mass spectrometry (GC/MS) via a modified EPA Method 8270. This analysis determined the concentrations of 62 parent and alkylated PAHs including sulfur-containing aromatics and 54 petroleum biomarkers (specifically, tricyclic and pentacyclic terpanes, regular and rearranged steranes, and triaromatic steroids). For calculating the sum of the PAH, nondetects were set to zero. The concentrations of target compounds presented herein are reported in ng/L (part-per-trillion, ppt) for both dissolved-phase and particulate/oil (filter) samples and are not surrogate-recovery corrected. Note that due to the typically low concentrations of hydrocarbons in water samples (versus tarballs or sediments), biomarkers were analyzed for only a small portion of water (particulate/oil phase) samples.
- Dispersant: the active surfactant ingredient in Corexit blends 9500 and 9527 is dioctyl-sulfosuccinate (DOSS). DOSS was analyzed in water samples by ALS Kelso (CAS) and various academic labs using a newly developed high-performance liquid chromatography/mass spectrometry (LCMS) method (Gray et al., 2011 and Kujawinski, et al. 2011). However, at Alpha Lab, standard GC/MS methods were used to semi-quantify Corexit indicator components (without reference standards): bis(2-ethylhexyl)fumerate (a DOSS-derived, GC injection port heat-breakdown product associated with both Corexit 9527 and 9500), 2-butoxyethanol (a major solvent in Corexit 9527) and di(propyleneglycol)-n-butyl ethers (designated as GE for glycol ethers in this report) and C_9-C_{14} petroleum distillates (the major solvents in Corexit 9500) (Stout, 2015). Concentrations presented herein are reported in ng/L (ppt) for both dissolved-phase and particulate/oil (filter) samples and are not surrogate-recovery corrected.
- Volatiles: a purge-and-trap method, modified EPA method 8260, was used to initially quantify a lengthy list of selected volatiles (PIANO) including aliphatic hydrocarbons from C_5 through C_{13} and C1-C5 alkyl-substituted benzenes and naphthalene (NOAA 2014). While not traditionally used for forensics analysis because of their ephemeral nature, many of these constituents are of interest because they are an important driver for toxicity. Later in the spill and at greater distances from the wellhead after many of these constituents were no longer being detected, the analyte list was trimmed. Only the standard BTEX analytes were most frequently detected and used exclusively for this report. BTEX constituents are reported in µg/L (ppb) in whole-water (non-filtered) samples only and are not surrogate-recovery corrected.

For phase-partitioned samples, dissolved-phase sample volumes were precisely measured during extraction to produce accurate concentration computations of both the dissolved and related particulate

(filter) samples. From lab storage, particulate (filter) samples were thawed, macerated, and extracted separately from the associated (dissolved) 3.5 L water portion.

All of the data have been validated by EcoChem as third-party validators; any exceedances were qualified during data validation. Publicly available data in NOAA DIVER are surrogate-recovery corrected; however, for the purpose of forensic analysis, recovery-correction of the data was not applied (termed the "forensic dataset"). A crosscheck of the forensic dataset with the publicly available data has shown the two datasets are equivalent differing only in the application of recovery correction to the public dataset.

Forensic Matching Categories

In establishing exposure to oil, traditional ASTM (2000) methods use match, indeterminate, or no-match categories to categories to describe forensic results. For exposure of water to DWH oil, a similar approach is taken, however, for however, for further understanding the oil's behavior and supporting the needs of SIMAP modelling, the match category match category is further subdivided into phase assignments, i.e., dissolved, particulate or indeterminate (undeterminable (undeterminable phase but matching MC252 oil). For reporting NRDA forensics samples, seven categories have become categories have become relevant to the case and SIMAP modeling (Table 1. Forensic Matching Categories for Water Samples

	Category Code	Comparable Category*	Description
Match	1	A	MC252—containing particulate phase (with or without extra dissolved)
	2		MC252—dissolved phase only
	3		MC252— phase uncertain, (irresolvably complex)
No Match	4	E	other oil or obvious ship-board contaminants (e.g., hydraulic fluid)
Indeterminate or clean	5	C	possible MC252 – oil-like profile but insufficient to link to MC252
	6	D	indeterminate—trace PAH detected but no oil-like profile
	7		no PAH detected or apparent noise (clean)

*Categories used in other reports on DWH forensics assessments of oil, tissues and sediment matrices.). The first three categories are each considered positive matches (consistent with MC-252 oil), differentiated by phase profiles. The remaining four are either other oil, inconclusive, or clean. Therefore, the product of this forensic evaluation was assignment of one of these categories to each water sample investigated. Forensic fingerprinting methods are described in a separate paper (Payne and Driskell, 2015a).

Table 1. Forensic Matching Categories for Water Samples

	Category Code	Comparable Category*	Description
Match	1	A	MC252—containing particulate phase (with or without extra dissolved)
	2		MC252—dissolved phase only
	3		MC252— phase uncertain, (irresolvably complex)
No Match	4	E	other oil or obvious ship-board contaminants (e.g., hydraulic fluid)
Indeterminate or clean	5	C	possible MC252 – oil-like profile but insufficient to link to MC252

	6	D	indeterminate—trace PAH detected but no oil-like profile
	7		no PAH detected or apparent noise (clean)

*Categories used in other reports on DWH forensics assessments of oil, tissues and sediment matrices.

Exposure

Surface Sampling

Four cruises with analytic chemistry results, the Response-directed, SMART dispersant-monitoring *International Peace*, NRDA Water Column TWG's *Bunny Bordelon* leg 1 and *Weatherbird II*, and BP/CSIRO directed *Ryan Chouest* legs 4-15 have been identified and reviewed as each having been specifically planned for off-shore, near-surface sampling. In addition, surface and near-surface samples were routinely collected as part of deeper casts on the NRDA cruises. Because of significant concern and interest in the near-surface zone of high biological productivity, the < 20 m water sample data were broken out and separately displayed (Figure 3) to show the extent of near-surface sampling and where positive matches to DWH oil were found. Care was taken to exclude samples that may have inadvertently included the surface-slick oil as a sampling artifact, and MC252 oil was confirmed in 359 out of 690 near-surface water samples for at least 100 km in most directions from the wellhead. Additional details (TPAH concentrations, depths, and range) on samples collected within 20 km of the wellhead are discussed below in a subsequent section titled Nearfield Dynamics.

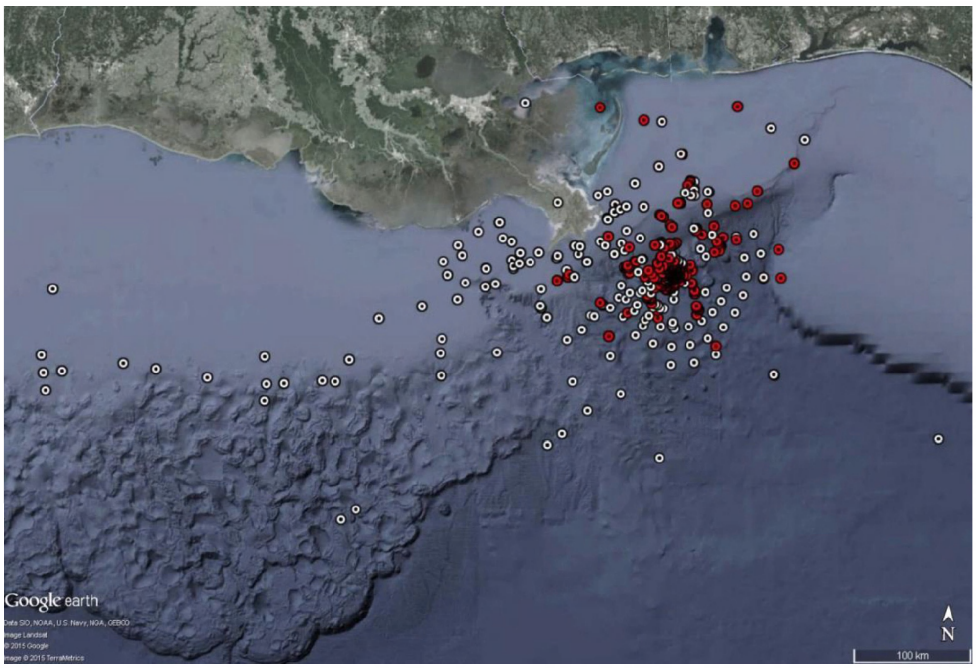

Figure 3. Near-surface (0-20m) forensic matches (red) and non-matches (white) (n=359 and 331, respectively).

Subsurface Sampling

The general results reflect each regime's physics and chemistry. Within the wellhead's nearfield, the rising plume creates a mix of whole-oil particulate droplets weathered by dissolution processes (described in opening section of this document and Payne and Driskell 2015a). The lingering dissolved components, rather than being advected away from the locale, may be transported by reversing currents back and forth

through the rising plume to create water parcels containing particulate profiles with extra dissolved portions. Similarly, at the air-sea interface, any droplet reaching the surface becomes part of the surface slick's amalgam of various weathered states plus any background contamination from vessels' exhaust, washes and bilge dumps, dispersant drops, or *in situ* burn operations.

Away from the rising plume, the water-washed, particulate droplets that have reached the surface begin losing additional lighter components through evaporative and photo-oxidation weathering processes in addition to continued dissolution back into the water column. With the requisite amount of wave energy, slicks can be mechanically broken up and surface droplets re-entrained in the upper depths (to some degree, 10-20 m, but more commonly 0-2 m). Data from SMART monitoring and *Bunny Bordelon* cruises demonstrate that surface-applied dispersants were also effective at creating micro-droplets that facilitated the dissolution, weathering, and re-entrainment processes (also see Payne and Driskell, 2015b).

In water samples, while all BTEX components are found as a mixture of oil-droplet-associated and truly-dissolved constituents in the deep samples near the wellhead, in the near-surface waters and further from the wellhead, benzene, the most volatile constituent of BTEX, is scarcer (Figure 4).

At depth, benzene could be observed at elevated concentrations (~20-40 µg/L) out to 15km, while the more persistent toluene was observed both at depth and in near-surface waters out to 100km. During the IXTOC oil well blowout in Mexico in 1979, similar selective benzene loss (dissolution) from the rising oil plume was reported from a depth of only 60 m (Payne, et al., 1980b). Other BTEX constituents generally appeared within 20km of the wellhead, and while most concentrated at depth, elevated concentrations of ethylbenzene and the xylenes could be observed out to 5-10 km from the wellhead from continued dissolution from rising oil droplets collecting near the surface (Figure 4 and Figure 5). As droplets reached the surface, any remaining BTEX constituents would be quickly lost to evaporation as was observed in air samples from above the wellhead (Ryerson et al. 2011).

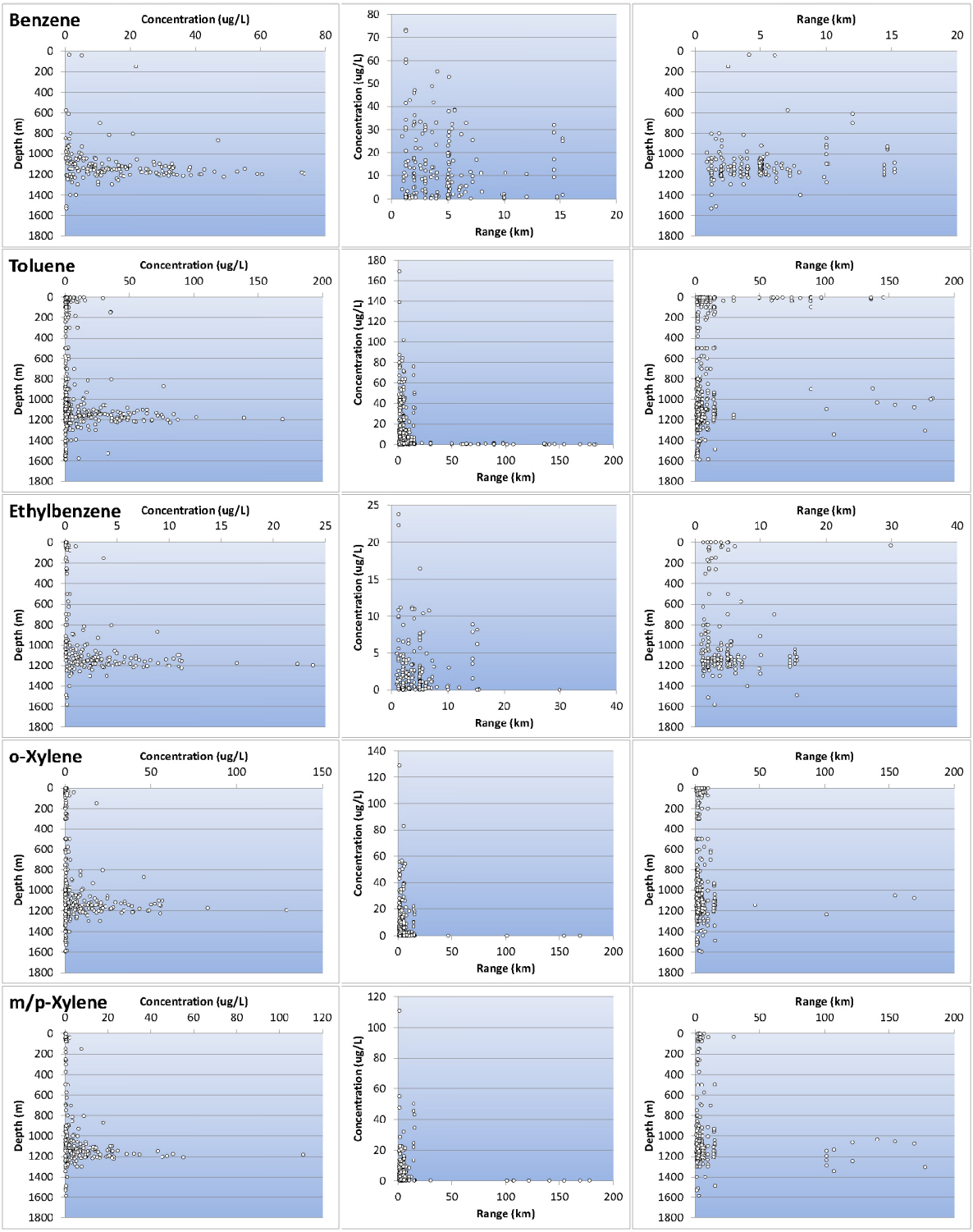

Figure 4. Distribution of BTEX in forensic-matched (category 1-3) samples by concentration (µg/L), depth (m) and range (km) from wellhead.

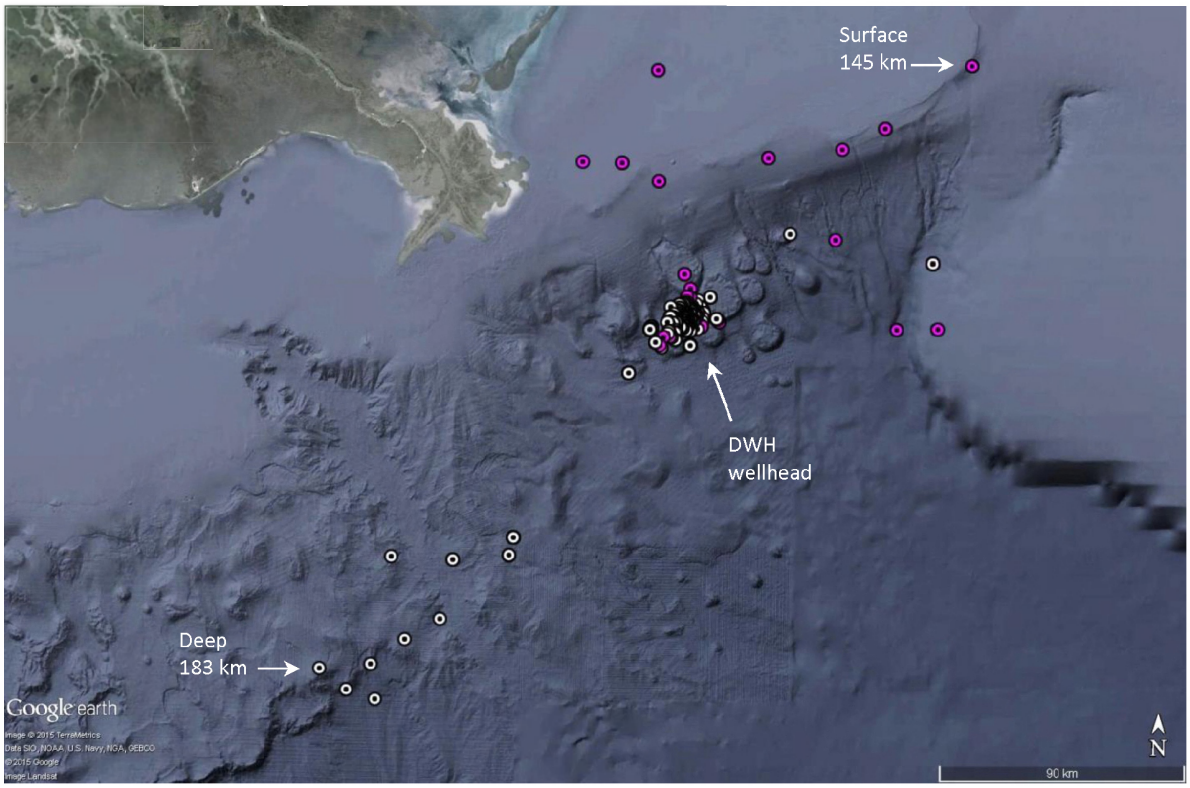

Figure 5. Distribution of surface and deep-plume, forensically-matched samples containing BTEX. Red dots are 0-20 m depth, white dots from greater than 800 m. Farthest surface sample NE at 145 km, deep plume sample SW at 183 km.

Forensic Matches

The primary deliverable from this study is a table of samples classified by forensic match categories (Table 1). Summary results show 45 cruises with 1,793 category 1-3 matches from 4,256 samples, not including field dups, blanks, and discarded samples (Table 2). Most concentrations were less than 100 part-per-trillion (ppt) for categories 1-3 (n=952) with category medians at 875, 177 and 30 ppt, respectively (Figure 6).

Table 2. Summary of the numbers of samples that were classified into each of the 7 categories, by cruise.

	Categories						
	Match			No Match	Indeterminate		
Study Name	weathered source (cat 1)	dissolved only (cat 2)	MC252 (cat 3)	other oil (cat 4)	Possible (cat 5)	Indeterminate (cat 6)	no PAH or noise (cat 7)
Brooks-McCall Cruise 02 MAY 15-17 2010	14	30	2		7	2	
Brooks-McCall Cruise 03 MAY 19-21 2010	8	22	1		3	13	
Brooks-McCall Cruise 04 MAY 23-25 2010	24	21	2		1		
Brooks-McCall Cruise 05 MAY 30-JUN 1 2010	32	29	3		2		3
Brooks-McCall Cruise 06 JUN 5-7 2010	32	15	13		9		6
Brooks-McCall Cruise 07 JUN 11-13 2010	33	21	23	2	2	11	4
Brooks-McCall Cruise 08 JUN 17-19 2010	11	17	18	6		36	7
Brooks-McCall Cruise 09 JUN 22-26 2010	13	46	12			8	9
Brooks-McCall Cruise 11 JUL 4-8 2010	12	11	12		5	7	9
Brooks-McCall Cruise 12 JUL 10-14 2010	23	20	11			23	20
Bunny Bordelon Cruise 01 MAY 30-JUN 2 2010	9	2	3		3	4	13
Endeavor Cruise 01 JUN 2010	10	7	24	4	10	4	44
Gordon Gunter Cruise 01 MAY 27-JUN 4 2010	29	20	9		3	43	42
Gordon Gunter Cruise 06 AUG 2-8 2010			5	1		1	53
Henry Bigelow Cruise 01 JUL 28-AUG 11 2010			7			23	36
Henry Bigelow Cruise 02 AUG 12-23 2010	1	2	71	2	29	4	282
HOS Davis Cruise 01 AUG 10-22 2010	7	9	16			4	17
HOS Davis Cruise 02 AUG 25-SEP 5 2010	1	10	31	2	4	15	1
HOS Davis Cruise 03 SEP 8-28 2010		1	74	40	2	29	48
HOS Davis Cruise 04 NOV 1-17 2010			37		15	50	45
HOS Davis Cruise 05 DEC 4-18 2010		10	8	7	1	4	15
Jack Fitz Cruise 01 MAY 9-14 2010	5	13	5	17	2	1	
Jack Fitz Cruise 02 MAY 21-31 2010	52	61	7	1	10	13	1
Jack Fitz Cruise 03 JUN 11-20 2010	12	38	15	2	7	23	1
Ocean Veritas Cruise 01 MAY 26-30 2010	8	1				10	1
Ocean Veritas Cruise 04 JUN 13-17 2010	23	9	24			13	
Ocean Veritas Cruise 05 JUN 19-23 2010		1	5				
Ocean Veritas Cruise 06 JUN 25-29 2010	5	3	20		2	46	4
Ocean Veritas Cruise 07 JUN 29-JUL 5 2010	18	14	25			31	34
Ocean Veritas Cruise 09 JUL 13-17 2010	8	6	34			32	22
Ocean Veritas Cruise 11 JUL 26-29 2010	5		18			47	11
Pisces Cruise 03 AUG 5-14 2010	1		7	1	6	4	107
Pisces Cruise 04 AUG 18-SEP 2 2010		1	88	2	2	34	122
Pisces Cruise 05 SEP 8-17 2010			19			2	27
Pisces Cruise 06 SEP 25-OCT 4 2010			5		1	2	7
Sarah Bordelon Cruise 07 DEC 4-19 2010			31	1		17	15

Seward Johnson Cruise 01 JUL 09-AUG 7 2010				1		1	72
Thomas Jefferson Cruise 02 JUN 3-10 2010	31	19	24	3	5	43	64
Thomas Jefferson Cruise 03 JUN 15-JUL 2 2010	8	18	13	1	3	38	212
Walton Smith Cruise 01 SEP 06-17 2010			21	1	1	4	13
Walton Smith Cruise 03 SEP 25-OCT 3 2010			12		9	6	67
Walton Smith Cruise 04 APR 19-MAY 27 2011						7	48
Water Sampling (R/V Intl Peace) 05-07/2010	45	38	29	1	13	1	47
Weatherbird II Cruise 01 MAY 06-15 2010	13						
Weatherbird II Cruise 02 MAY 23-26 2010	1	1		3	3	14	5
totals	494	515	784	98	160	670	1534
	11.61%	12.10%	18.42%	2.30%	3.76%	15.74%	36.04%

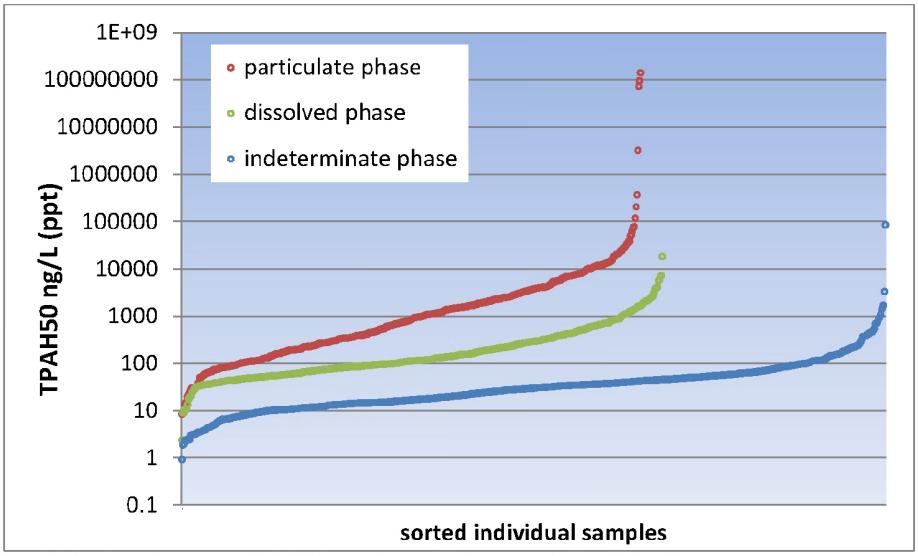

Figure 6. Sorted TPAH distributions of MC-252 matches (Categories 1-3), all depths.

Although the depth and location of each individual sample were used during the forensic identification process, full temporal and spatial pattern interpretations are being left to the modelers. However, obvious from this data review, at the entrapped plume depth, there is a trail of particulate-phase (categ. 1) samples out to 155 km from the wellhead, while dissolved-profile (categ. 2) samples, typically with dispersant indicators, ranged to 267 km SW from the wellhead, and indeterminate-phase (categ. 3) samples to 412 km from the wellhead (Figure 7). Dispersant-mediated samples extended out to 184 km to the SW within the deepwater plume and up to 148 km to the NE with the surface water (< 20 m) atop the shelf (Figure 8). The entrapped deepwater plume is partially defined by the non-matches with bounding samples out to 530 km along the continental shelf break and 437 km along the plume track from the wellhead (Figure 9). These data categories are best portrayed in 3-dimensional plots clearly delineating the deep plume (Figure 10).

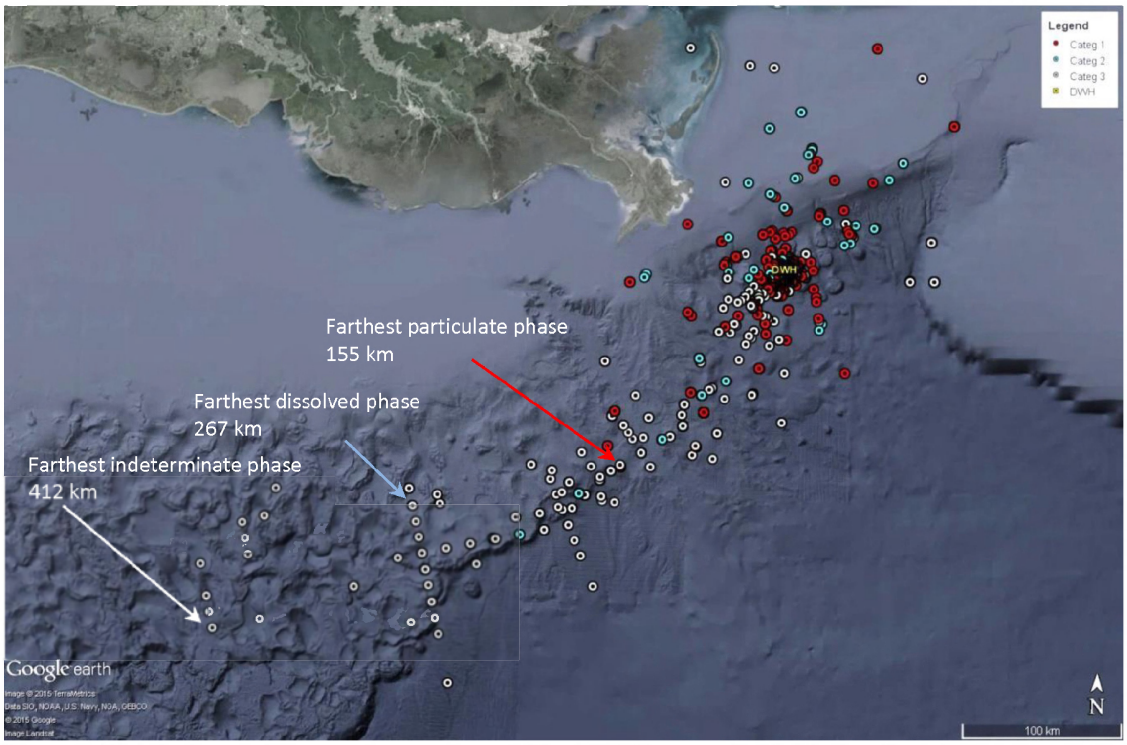

Figure 7. Distribution of offshore water samples matching MC252 source oil. Matched particulate (Cat. 1; red), dissolved (Cat. 2; blue), and indeterminate phase (Cat. 3; white) samples range to 155, 267, and 412 km from wellhead, respectively. Each location may have multiple depths. n=1,768 matches.

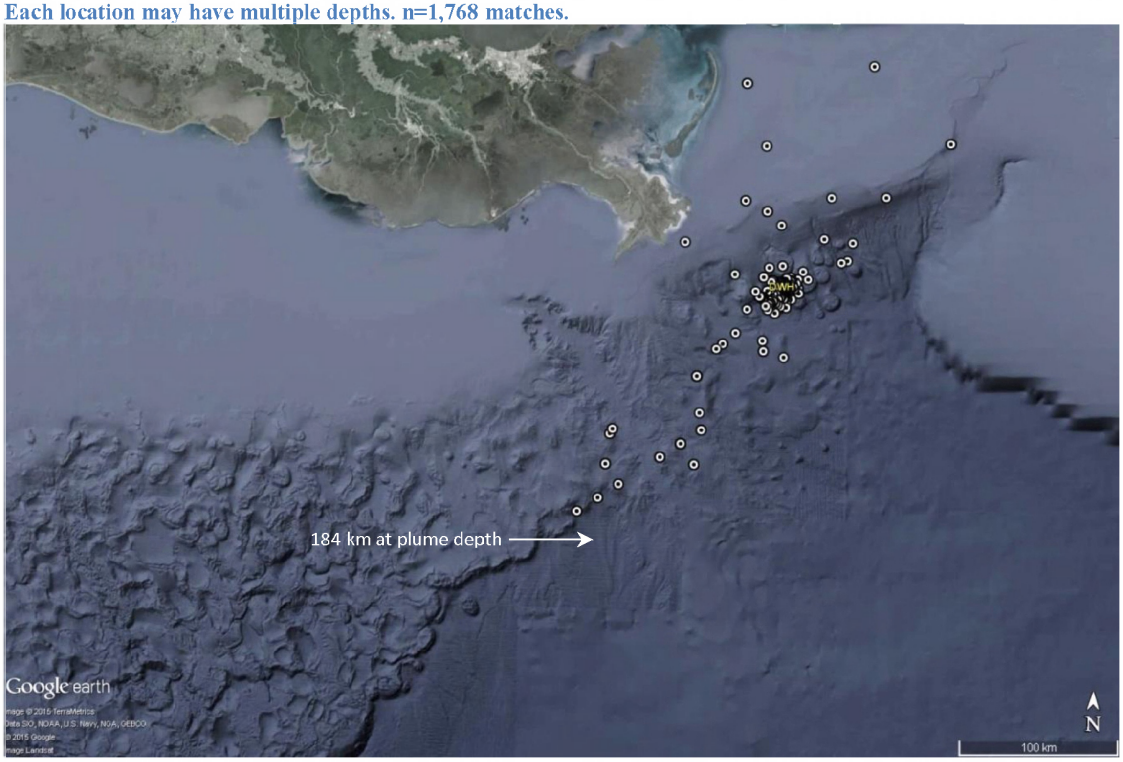

Figure 8. Distribution of dispersant-mediated samples matching MC252 source oil. Samples to the SW of the wellhead were at deep plume depth. Samples on shelf NE of wellhead were from <20m depth.

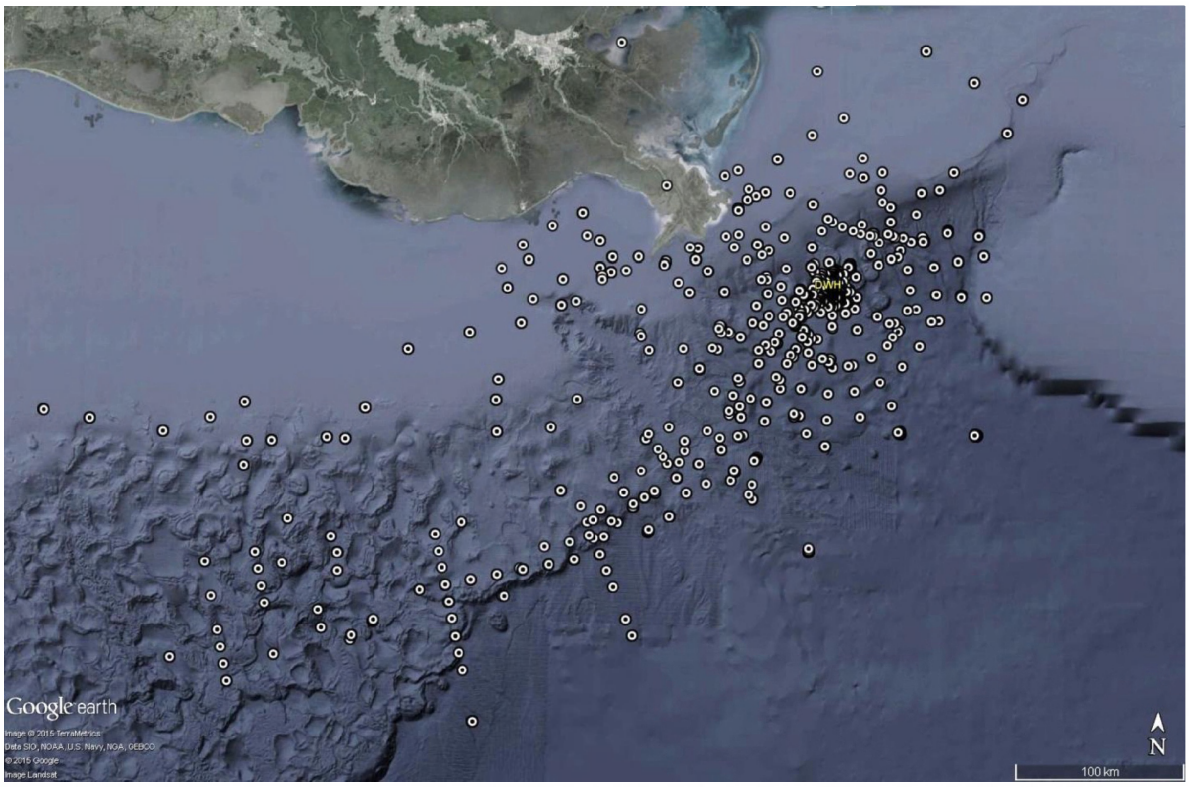

Figure 9. Distribution of samples not matching MC-252 (categories 4-7) ranging to 530 km from wellhead. All depths. n=2,443.

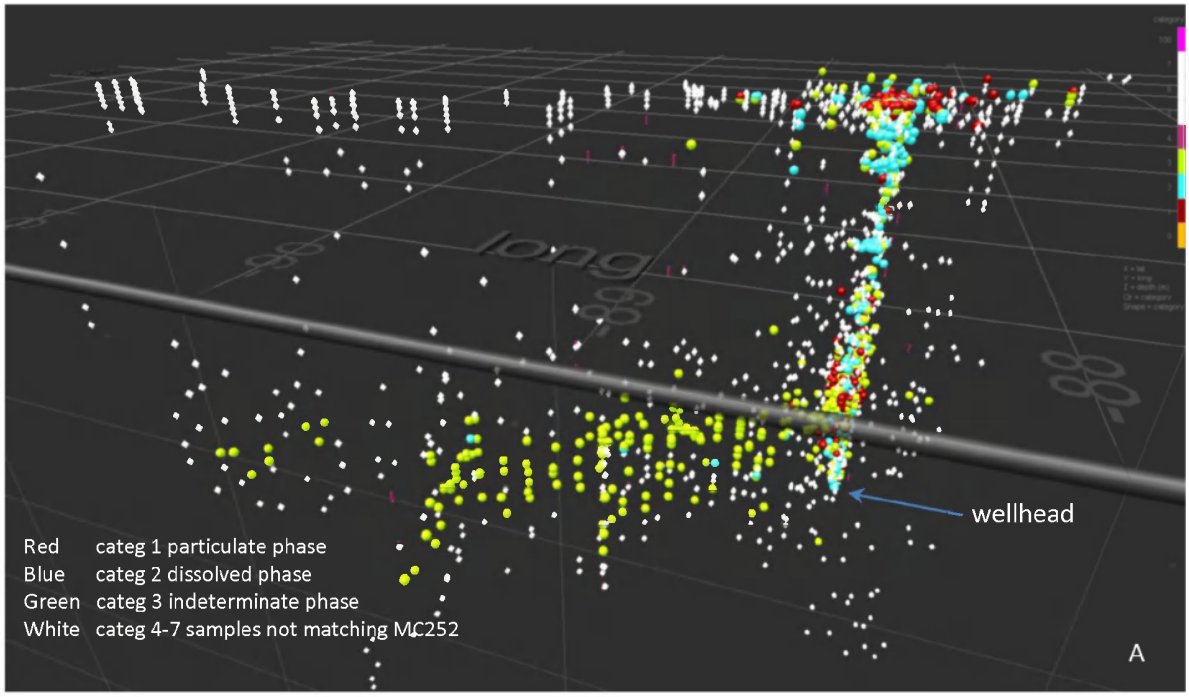

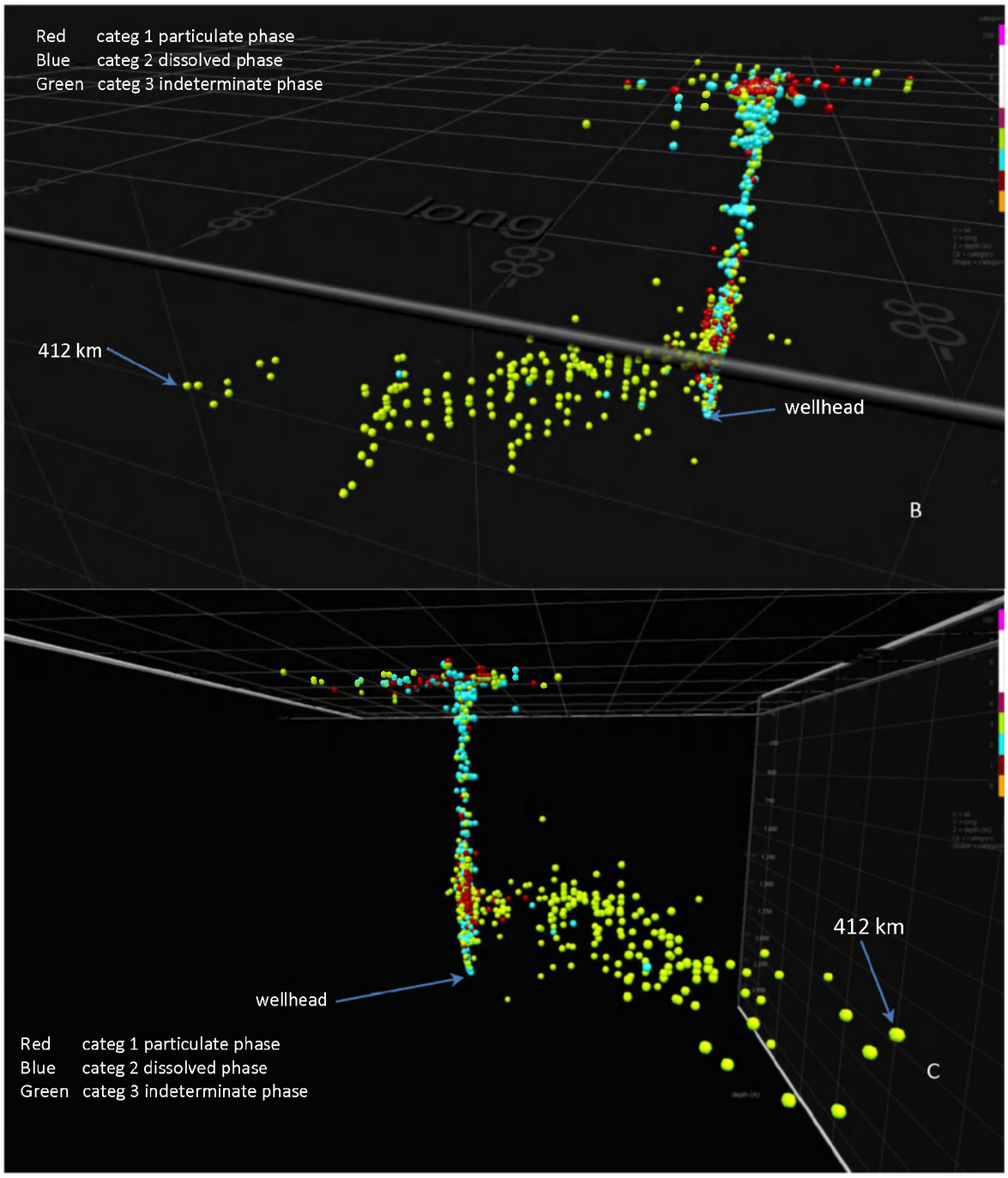
Red categ 1 particulate phase
Blue categ 2 dissolved phase
Green categ 3 indeterminate phase
long
412 km
wellhead
B
412 km
wellhead
C
Red categ 1 particulate phase
Blue categ 2 dissolved phase
Green categ 3 indeterminate phase

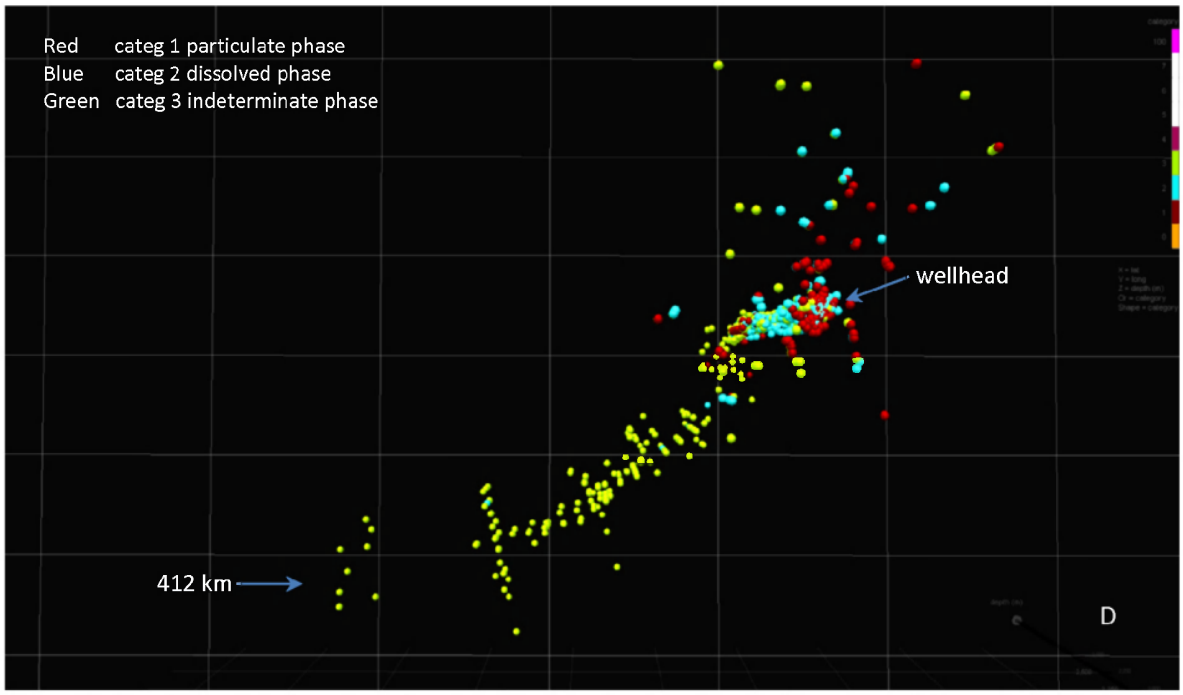

Figure 10. Four 3D spatial views of samples colored by forensic categories. A) oblique view of all samples looking north (column of blue is rising plume near wellhead) B) view A with only matched samples displayed, C) at plume depth looking NE from beyond plume's end (500 km), D) top view from above wellhead.

Nearfield dynamics

From forensic data, there is no structured "cone" above the wellhead defining the rising plume of gases and particulate oil droplets. Rather, the rising hydrocarbons were subject to ever shifting displacement as water parcels at each depth were subjected to turbulence, tidal currents and basin circulation (see modeling reports). The forensic data support this scenario. Three-dimensional plots of water samples with particulate-phase oil (category 1 samples with droplets rising above the ~1000m entrapment layer) lack any discernible cone-shape distribution within 20km of the wellhead (Figure 11A). Adding category 3 samples containing an unparseable phase profile but with confirmed particulate oil, the distribution is filled in but still with no cone appearing (Figure 11B). Adding category 2, dissolved phase samples demonstrate that within the same space where droplets were encountered, dissolved- phase-only samples were collected (Figure 11C). These hydrocarbons were dissolved out of the droplets as they ascended, remaining behind as residual tracers but now shifting with the moving parcels of water. Finally, samples lacking detectible oil (category 5-7) were also uniformly distributed throughout the same nearfield space suggesting the absence of a static or near-static cone as a feature of the rising plume (Figure 11D). These data appear to fit well with conceptual rising plume processes as depicted by ASA (Figure 12).

TPAH50 values for confirmed matches show remarkable similarities within depths for the varying ranges (Figure 13 and Table 3) but note that the upper depths (above 800m) comprise only ~140 samples (vs. 1026 deepwater plume-related samples). Maximum values were found in closer proximity to the well. Below 800m, half the samples were ~<100 ppt while a few higher concentration samples from within 5 km raised the average to ~11,000-15,000 ppt.

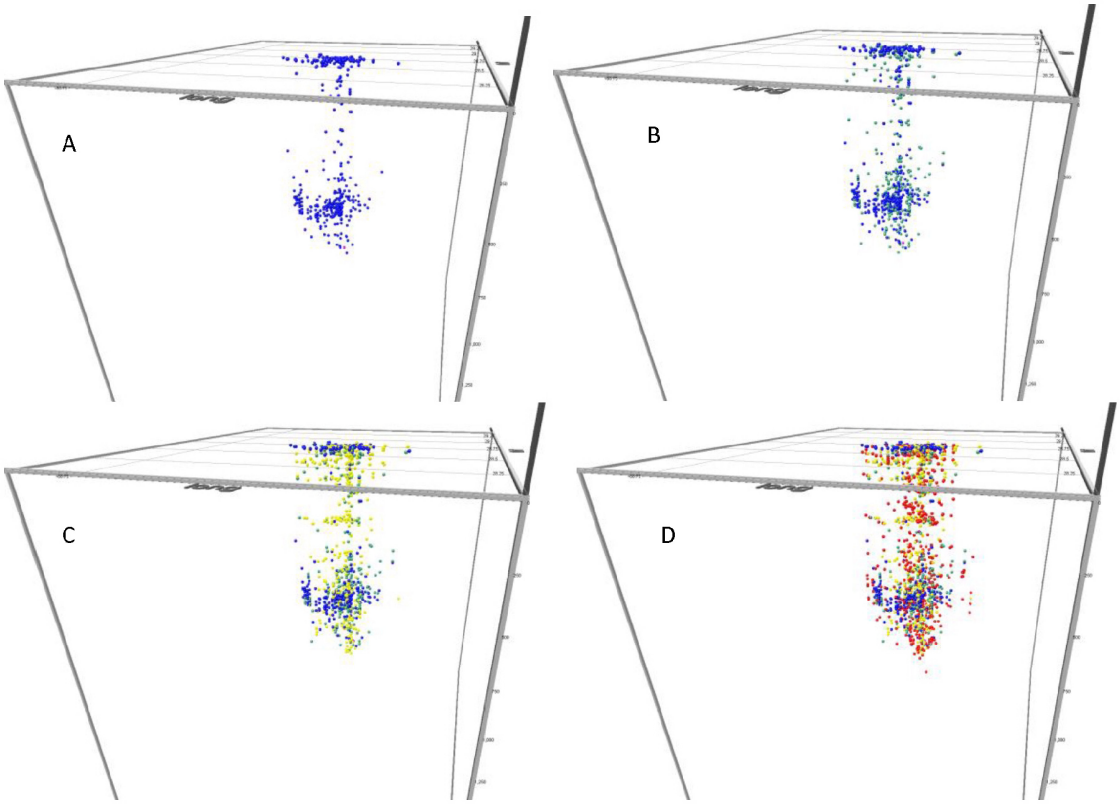

Figure 11. Distribution of forensically reviewed samples within 20km of wellhead. A) Category 1 samples (blue) containing particulate oil (droplets) were primarily encountered at the surface and at plume depth. B) Adding category 3 samples (green), unparseable phase but also with particulate oil. C) Category 2 (yellow), dissolved phase samples show where droplets weren't encountered. D) Category 5-7 samples (red) show where oil wasn't encountered, within the same but not defining a static rising plume (n=2198 within 20km radius). View is facing north.

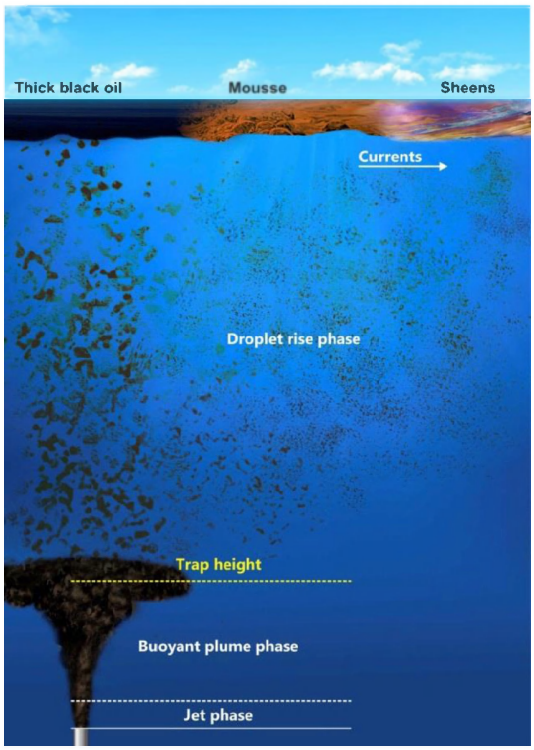

Figure 12. Conceptual depiction of rising plume and trap layer (from French-McKay, 2015).

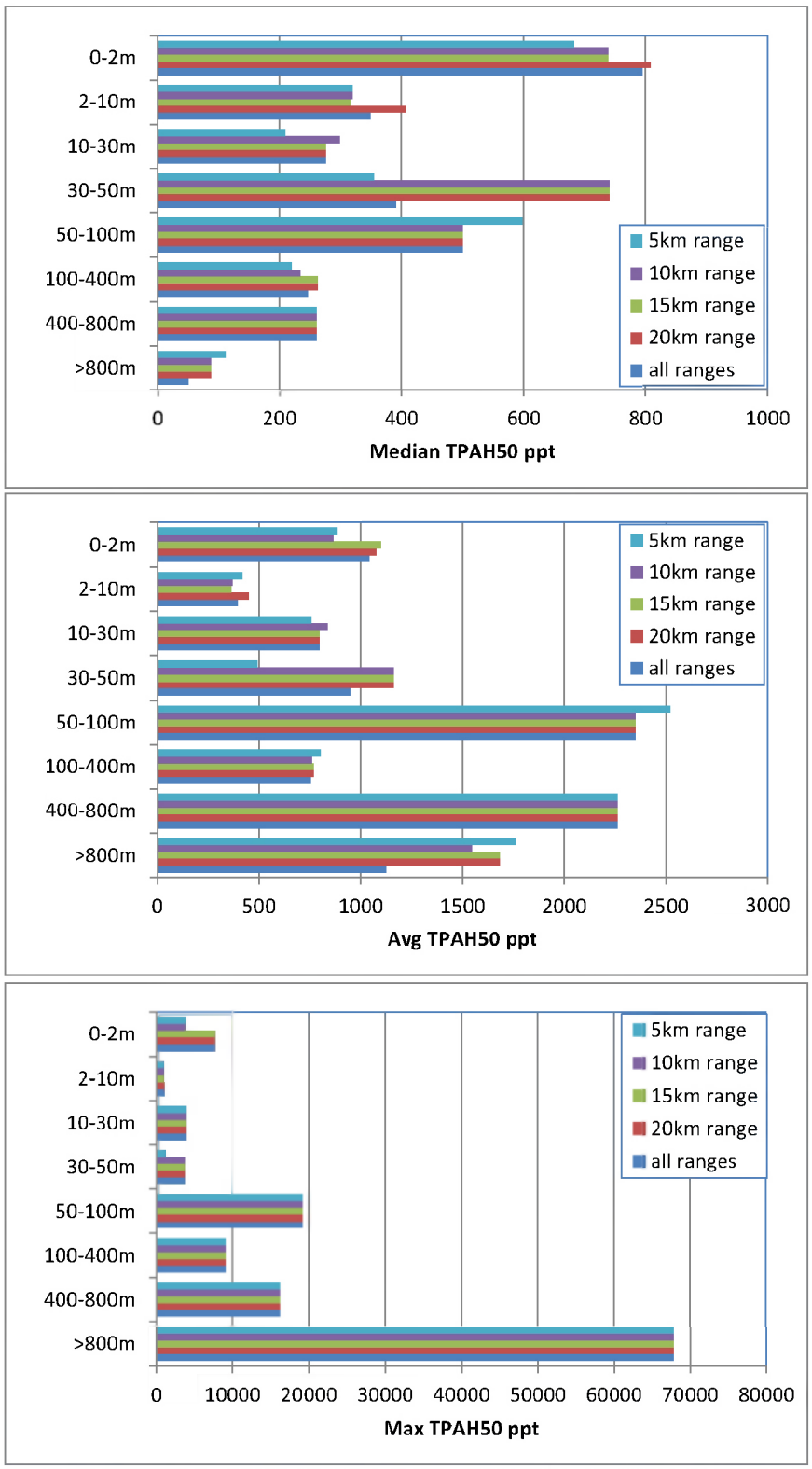

Figure 13. TPAH50 summaries of various depths and radii from the wellhead. Maximum concentration samples were generally found closer to the wellhead.

Table 3. TPAH50 (ng/L, ppt) values for forensically confirmed (category 1-3) samples grouped by parameter, range and depth (from above plots).

Median TPAH50 ppt	0-2m	2-10m	10-30m	30-50m	50-100m	100-400m	400-800m	>800m
all km range	795	350	276	391	500	248	262	51
20km range	808	408	276	741	500	263	262	88
15km range	739	317	276	741	500	263	262	88
10km range	739	320	299	741	500	234	262	89
5km range	682	320	210	356	598	221	262	111
Average TPAH50 ppt								
all km range	1042	395	797	950	2349	756	2264	1124
20km range	1078	451	797	1165	2349	770	2264	1682
15km range	1101	363	797	1165	2349	770	2264	1682
10km range	868	371	837	1165	2349	763	2264	1545
5km range	887	418	759	492	2520	804	2264	1763
Max TPAH50 ppt								
all km range	7760	1119	3994	3649	19150	9017	16156	67792
20km range	7760	1119	3994	3649	19150	9017	16156	67792
15km range	7760	998	3994	3649	19150	9017	16156	67792
10km range	3821	998	3994	3649	19150	9017	16156	67792
5km range	3821	998	3994	1261	19150	9017	16156	67792
Count of samples								
all km range	31	14	17	10	14	47	9	1026
20km range	29	10	17	8	14	46	9	679
15km range	24	7	17	8	14	46	9	653
10km range	20	6	16	8	14	44	9	587
5km range	15	4	14	6	13	41	9	438

Sampling Effectiveness

There have been concerns expressed that the predominance of "low" TPAH values reported from all water column chemistry results suggests low exposure and thus, from an injury point of view, only limited potential impacts on Gulf resources. Without invoking toxicology results, these concerns are best addressed by breaking the data into three groups: 1) the nearfield plume rising from wellhead to the surface, 2) the entrapped deepwater oil plume advected at depth from the wellhead, and 3) surface waters (<20m). First, the nearfield plume was well sampled and contained high TPAH values. Most early cruises focused their efforts within the salt-dome-encircled basin surrounding MC-252 and as close to the wellhead as on-going response operations would allow. Included in the efforts were some systematic sampling schemes to define extent of exposure. As expected, high concentration samples were common within the nearfield zone.

At depth, outside the nearfield zone, as stated earlier in this document, the data represent only exploratory spatial and temporal snapshots of spill conditions taken under a scheme to find and track the deepwater oil plume. Indeterminate and non-matching category samples (categ. 5-7) were expected, even desired as they define the plume boundaries (see white-coded samples in Figure 10A) and provide evidence that

sampling/procedural artifacts (e.g., equipment contamination, categ. 4) was not a major problem during the field effort. Furthermore, even if a multi-bottle cast intercepted the deep plume, only a few of the samples might be taken within the plume. In summary, these data do not represent the complete universe of oiling in the water column; that is the task of modeling.

Exposure values from within the plume are also biased in the sense that they only represent the detectable concentrations of target analytes, the "visible PAH." Recent work has shown that our GC/MS view of hydrocarbons, while reliable and prodigiously productive, has constrained ability to show that transformative weathering processes don't obliterate the plume, it just becomes less visible (see additional discussion in Appendix 1 of this report). Our TPAH50 values only reflect the target analytes amenable to our instruments and methods—those that we can measure. Using alternative methods (FT-ICR instruments), McKenna et al. (2013) have identified more than 30,000 hydrocarbon compounds in Macondo oil, while Aeppli et al., 2012, and Ruddy et al. 2014, among others, have documented advanced oxidation states in slicks and stranded tarballs due to photo-oxidation and shoreline weathering. Although the water column samples have not yet been analyzed using these methods, it is highly likely that some fraction of the residual deep plume constituents were microbially converted into similar polar products (Gutierrez et al., 2013a,b and Appendix 1). Unquantified polar derivatives would be a logical explanation for the most distant category 3 sample at 412km which had none of the relevant target PAH but all of the other indicators of the deepwater plume (fluorescence, DO, and dispersant indicators) (discussed further in Appendix 1). Past research following the *Exxon Valdez* oil spill also suggested enhanced toxicity for weathered oil products (Carls et al., 1999; Incardona, et al., 2004, 2005).

Lastly, near-surface sampling efforts (<20m) detailed the exposure in a zone of high productivity and of high concern but were secondary to the then undocumented deep plume behavior and deep-sea weathering. Consequently, forensically reviewed near-surface samples represented only ~18% of this data set (Figure 3 and Figure 14). At depth, the 808 matches in the deepwater plume empirically define the plume's boundaries (~1000-1400m, where hits occurred frequently) but the higher frequencies are also a result of the focused sampling, i.e., when sensors suggested the plume was detected, the sampling often bracketed the depths. Similarly, the plateau at 500 m partially results from a propensity to systematically sample at that depth rather than a frequently occurring feature.

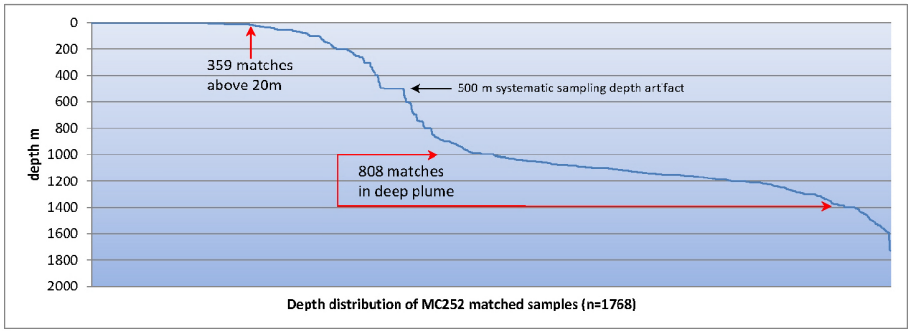

Figure 14. Depth distribution of matched samples (n=1768) reflecting both oil encounter and sampling intensity.

Two studies conceived to look at oil concentrations below slicks and at dispersant effects, SMART monitoring aboard the *International Peace* and the *Bunny Bordelon*, both found that while there was evidence of enhanced dissolution of PAH due to dispersant applications, TPAH concentrations rapidly dropped off (order of magnitude) in the top ~10m. A third set, independent BP/CSIRO cruises, found similar low-level effects in fluorometry down to 10-20m depth. A fourth NRDA study, the *Weatherbird II,* collected some slick and shallow water samples on its tracks through the eastern region of the spill.

Taken together, these data would suggest that finding significant particulate-oil concentrations at even slightly deeper depths would require 1) a rising wellhead plume or 2) chemically dispersed micro-droplets, and/or 3) major turbulence to re-entrain surface oil (storm waves). The first two conditions were to a degree, covered by NRDA sampling while the third was operationally impossible due to safety constraints using available methods.

Finally, 42 (1.8%) of the water samples contained oil that did not matched to MC252 (Category 4). Most (25) were due to hydraulic oil leaked from the ROVs. The other 17 represented other obvious but unidentified contaminants or were from unknown sources.

Conclusions

After forensically examining 5,332 offshore water samples from early NRDA field collections, MC252 oil has been detected at depth, weathering-state discriminated, and characterized for dispersant effects. Dispersant indicators, measured for the first time in field-collected, particulate-phase oil samples at depth, document the utility of dispersant injections at the wellhead for reducing oil-droplet sizes and thus, limiting oil rising to the surface and potentially being transported to shorelines (detailed in Payne and Driskell, 2015b). Dispersant application at depth also resulted in significantly enhanced dissolution of lower- and intermediate-molecular weight PAH contributing to enhanced bioavailability to both benthic and pelagic organisms.

MC252 oil has been identified in subsurface water samples as particulate-phase hydrocarbons up to 155 km from the wellhead, and as dissolved-phase as far as 267 km from the wellhead. Furthermore, based solely on dispersant indicators, fluorescence and DO features, the presence of the plume was detected 412 km from the wellhead (Figure 7). It follows from other oil-weathering studies (McKenna et al. 2013, Aeppli et al. 2012, Ruddy et al. 2014), that oxygenated hydrocarbons, polar derivatives not detectible using standard GC/MS methods, may still be present in unknown concentrations in this distant plume. Helping define plume boundaries, non-matching (clean, Category 5-7) samples were taken from various depths and directions up to 530km from the wellhead (Figure 9 and Figure 10A)

References

Aeppli, C., C.A. Carmichael, R.K. Nelson, K.L, Lemkau, W.M. Graham, M.C. Redmond, D.L. Valentine, and C.M. Reddy. (2012). Oil weathering after the Deepwater Horizon disaster led to the formation of oxygenated residues. *Environ. Sci. Technol.* 46: 8799-8807.

Allan, S.E., B.W. Smith, and K.A. Anderson. (2012). Impact of the Deepwater Horizon oil spill on bioavailable polycyclic aromatic hydrocarbons in Gulf of Mexico coastal waters. *Environ. Sci. Technol.* 46: 2033-2039.

ASTM D 5739-00 (2000). Standard practice for Oil Spill Source Identification by gas chromatography and positive ion electron impact low resolution mass spectrometry. ASTM International, 100 Barr Harbor Drive, P.O. Box C700, West Conshohocken, PA 19428-2959.

Boehm, P.D. and D.L. Fiest. (1982). Subsurface distributions of petroleum from an offshore well blowout: The IXTOC 1 blowout, Bay of Campeche. *Environ. Sci. Technol* 16: 67-74.

Boehm, P.D., L.L. Cook and K.J. Murray. (2011). Aromatic hydrocarbon concentrations in seawater: Deepwater Horizon oil spill. *Proceedings of the 2011 International Oil Spill Conference*, American Petroleum Institute, Washington, D.C.

Brandvik, P.J., Ø. Johansen, F. Leirvik, U. Farooq, P.S. Daling. (2013). Droplet breakup in subsurface oil releases – Part 1: Experimental study of droplet breakup and effectiveness of dispersant injection. *Marine Pollution Bulletin* 73(1): 319-326.

Camilli, R., C.M. Reddy, D.R. Yoerger, B.A.S. VanMooy, M.V. Jakuba, J.C. Linsey, C.P. McIntyre, S. P. Sylva, and J.V. Maloney. (2010). Tracking hydrocarbon plume transport and biodegradation at the Deepwater Horizon. *Science* 330:201-204.

Camilli R, D. Di Iorio, A. Bowen, C.M. Reddy, A.H. Techet, D.R. Yoerger, L.L. Whitcomb, J.S. Seewald, S.P. Sylva, and J. Fenwick. (2011). Acoustic measurement of the Deepwater Horizon Macondo well flow rate. *Proceedings of the National Academy of Sciences,* doI: 10.1073/pnas 110038108.

Campo, P., A.D. Venosa, and M.T. Suidan (2013). Biodegradability of Corexit 9500 and dispersed South Louisiana crudc oil at 5 and 25° C. *Environ. Sci. Technol.* 47: 1960-1967.

Carls, M.G., S.D. Rice, J.E. Hose. (1999). Sensitivity of fish embryos to weathered crude oil: Part I. Low-level exposure during incubation causes malformations, genetic damage, and mortality in larval Pacific herring (*Clupea pallasi*). *Environ. Toxicol. Chem.* 18, 481-493.

Crespo-Medina, M., C.D. Meille, K.S. Hunter, A.R. Diercks, V.L. Asper, V.J. Orphan, P.L. Tavormina, L.M. Nigro, J.J. Battles, J.P. Chanton, A.M. Shiller, D.J. Joung, R.M.W. Amon, A. Bracco, J.P. Montoya, T.A. Villareal, A.M. Wood, and S.B. Joye. (2014). The rise and fall of methanotrophy following a deepwater oil-well blowout. *Nature Geoscience* 7: 423-427. .

Diercks ARH, R.C.; V.L.Asper, D. Joung, Z. Zhou, L. Guo, A.M. Shiller, S.B. Joye, A.P. Teske, N. Guinasso, T.L. Wade, and S.E. Lohrenz. (2010). Characterization of subsurface polycyclic aromatic hydrocarbons at the Deepwater Horizon site. *Geophys. Res. Lett.* 37: L20602.

Douglas, G.S., A.E. Bence, R.C. Prince, S.J. McMillen, and E.L. Butler. (1996). Environmental stability of selected petroleum hydrocarbon source and weathering ratios. *Environ, Sci. Technol.* 30(7): 2332-2339.

Driskell, W.B., J.R. Payne and G.C. Douglas, 2010. Forensic fingerprinting of *Cosco Busan* samples containing mixed-oil sources. Presentation at the Society of Environmental Toxicology and Chemistry, Special session on the Cosco Busan Spill. SEATAC 31st Annual Meeting, November 7-10, 2010. Portland, OR.

Du, M. and J.D. Kessler. (2012). Assessment of the spatial and temporal variability of bulk hydrocarbon respiration following the Deepwater Horizon oil spill. *Environ. Sci. Technol.* 46: 10499-10507.

Edwards, B.R., C.M. Reddy, R. Camilli, C.A. Carmichael, K. Longnecker, and B.A.S. Van Mooy. (2011). Rapid microbial respiration of oil from the Deepwater Horizon spill in offshore surface waters of the Gulf of Mexico. *Environ. Res. Lett.* 6: 035301.

Faksness, Liv-Guri (2007). Weathering of oil under Arctic conditions: Distribution and toxicity of water soluble oil components dissolving in seawater and migrating through sea ice. A combined laboratory and field study. Ph.D. Dissertation at the University of Bergen & the University Centre in Svalbard. 152 pp.

French McCay, D.P, K. Jayko, Z. Li, M. Horn, Y. Kim, T. Isaji, D. Crowley, M. Spaulding, S. Zamorski, J. Fontenault, R. Shmookler, and J.J. Rowe, 2015a. Technical Reports for Deepwater Horizon Water Column Injury Assessment – WC_TR.14: Modeling Oil Fate and Exposure Concentrations in the Deepwater Plume and Rising Oil Resulting from the Deepwater Horizon Oil Spill. RPS ASA, South Kingstown, RI, USA, August 2015.

Gray, J.L., L.K. Kanagy, E.T. Furlong, J.W. McCoy, and C.J. Kanagy. (2011). Determination of the anionic surfactant di(ethylhexyl)sodium sulfosuccinate in water samples collected from Gulf of Mexico coastal waters before and after landfall of oil from the Deepwater Horizon oil spill, May to October, 2010. U.S. Geological Survey Open-File Report 2010-1318, 15 p <http://www.pubs.usgs.gov/of/2010/1318/>

Gray, J.L., L.K. Kanagy, E.T. Furlong, C.J. Kanagy, J.W. McCoy, A. Mason, and G. Lauenstein. (2014). Presence of the Corexit component dioctyl sodium sulfosuccinate in Gulf of Mexico waters after the 2010 Deepwater Horizon oil spill. *Chemosphere* 95: 124-130.

Gutierrez, T., D. Berry, T. Yang, S. Mishamandani, L. McCKay, A. Teske, and M.D. Aitken. (2013a). Role of bacterial exopolysaccharides (EPS) in the fate of the oil released during the Deepwater Horizon oil spill. PLOS ONE 8(6): e67717

Gutierrez, T., D.R. Singleton, D. Berry, T. Yang, M.D. Aitken, and A. Teske. (2013b). Hydrocarbon-degrading bacteria enriched by the Deepwater Horizon oil spill identified by cultivation and DNA-AIP. ISME Journal, 7, 2091-2104. Doi: 10.1038/ismej. 2013.98.

Hall, G.J., G.S. Frysinger, C. Aeppli, C.A. Carmichael, J. Gros, K.L. Lemkau, R.K. Nelson, C.M. Reddy. (2013). Oxygenated weathering products of Deepwater Horizon oil come from surprising precursors, *Marine Pollution Bulletin*, 75 (1-2): 140-149.

Hazen T.C., E.A. Dubinsky, T.Z. DeSantis *et al.* (2010) Deep-sea oil plume enriches indigenous oil-degrading bacteria. *Science* 330: 204-208.

Incardona, J.P., T.K. Collier, N.L. Scholz. (2004). Defects in cardiac function precede morphological abnormalities in fish embryos exposed to polycyclic aromatic hydrocarbons. *Toxicol. Appl. Pharmacol.* 196, 191-205.

Incardona, J.P., M.G. Carls, H. Teraoka, C.A. Sloan, T.K. Collier, N.L. Scholz. (2005). Aryl hydrocarbon receptor-independent toxicity of weathered crude oil during fish development. *Environ. Health Perspect.* 113, 1755-1762.

Incardona, J.P, T.L. Swarts, R.C. Edmunds, T.L. Linbo, A. Aquilina-Beck, C.A. Sloan, L.D. Gardner, B.A. Block, N.L. Scholz. (2013). Exxon Valdez to Deepwater Horizon: Comparable toxicity of both crude oils to fish early life stages, *Aquatic Toxicology* Vol. 142–143: 303-316.

Johansen, Ø, P.J. Brandvik, U. Farooq. (2013). Droplet breakup in subsea oil releases – Part 2: Predictions of droplet size distributions with and without injection of chemical dispersants. *Marine Pollution Bulletin*, 73(1): 327-335.

Katz, J. (2009). Measurements and modeling of size distributions, settling, and dispersions (turbulent diffusion) rates. Final Report prepared for the Coastal Response Research Center. August 2009. 31 pp.

Kujawinski, E.B., M.C.K. Soule, D.L. Valentine, A.K. Boysen, K. Longnecker, and M.C. Redmond. (2011). Fate of dispersants associated with the Deepwater Horizon oil spill. *Environ. Sci. Technol.* 45(5): 1298-1306.

Li, Z., A. Bird, J. Payne, N. Vinhateiro, and Y. Kim. (2013). Draft physical-chemical technical reports for Deepwater Horizon Water Column Trustees: Volume III. Oil particle data from the Deepwater Horizon oil spill. RPS ASA 55 Village Square Drive, South Kingstown, RI 02879.

Liu, Z., J. Liu, W.S. Gardner, G.C. Shank, N.E. Ostrom, (2014). The impact of Deepwater Horizon oil spill on petroleum hydrocarbons in surface waters of the northern Gulf of Mexico, *Deep Sea Research Part II: Topical Studies in Oceanography*, Available online 23 January 2014,

Lubchenco, J., M.K. McNutt, G. Dreyfusa, S.A. Murawskia, D.M. Kennedy, P.T. Anastas, S. Chu, and T. Hunter. (2012). Science in support of the Deepwater Horizon response. *Proceedings of the National Academy of Sciences 109(50):* 20212–20221.

Mariano, A.J., V.H. Kourafalou, A. Srinivasan, H. Kang, G.R. Halliwell, E.H. Ryan, and M. Roffer. (2011). On the modeling of the 2010 Gulf of Mexico Oil Spill. Dynamics of Atmospheres and Oceans 52: 322-340.

McAuliffe, C.D. (1987). Organism exposure to volatile/soluble hydrocarbons from crude oil spills – a field and laboratory comparison. *Proceedings of the 1987 International Oil Spill Conference*, American Petroleum Institute, Washington, D.C., pp. 275-288.

McKenna, A.M., R.K. Nelson, C.M. Reddy, J.J. Savory, N.K. Kaiser, J.E. Fitzsimmons, A.G. Marshall, and R.P. Rodgers. (2013). Expansion of the analytical window for oil spill characterization by ultrahigh resolution mass spectrometry: Beyond gas chromatography. *Environ. Sci. Technol.* 47: 7530-7539.

McNutt, M, R. Camilli, G. Guthrie *et al.* (2011) Assessment of Flow Rate Estimates for the Deepwater Horizon / Macondo Well Oil Spill. Flow Rate Technical Group report to the National Incident Command, Interagency Solutions Group, March 10, 2011.

McNutt M.K., S. Chu, J. Lubchenco, T. Hunter, G. Dreyfus, S.A. Murawski, and D.M. Kennedy. (2012) Applications of science and engineering to quantify and control the Deepwater Horizon oil spill. *Proceedings of the National Academy of Sciences* 109: 20222-20228.

National Research Council (NRC). (1985). Oil in the Sea: Inputs, Rates, and Effects. National Academy Press, Washington, D.C.

National Research Council (NRC). (1989). Using Oil Spill Dispersants on the Sea. National Academy Press, Washington, D.C.

National Research Council (NRC). (2003). Oil in the Sea III: Inputs, Rates, and Effects. National Academy Press, Washington, D.C.

National Research Council (NRC). (2005). Oil Spill Dispersants: Efficacy and Effects. National Academy Press, Washington D.C., 377 pp.

NOAA. 2014. Analytical quality assurance plan, Mississippi Canyon 252 (Deepwater Horizon) natural resource damage assessment, Version 4.0. May 30, 2014.

Passow, U., K. Ziervogel, V. Asper, and A. Diercks. (2012). Marine snow formation in the aftermath of the Deepwater Horizon oil spill in the Gulf of Mexico. *Environ. Res. Lett.* 7. 11 pp.

Payne, J.R., G.S. Smith, P.J. Mankiewicz, R.F. Shokes, N.W. Flynn, W. Moreno and J. Altamirano. (1980a). Horizontal and vertical transport of dissolved and particulate-bound higher-molecular-weight hydrocarbons from the IXTOC I blowout. Proceedings: Symposium on Preliminary Results from the September 1979 RESEARCHER/PIERCE IXTOC I Cruise. June 9-10, 1980, Key Biscayne, Florida. pp. 119-166. NTIS Accession Number PB81-246068.

Payne, J.R., N.W. Flynn, P.J. Mankiewicz, and G.S. Smith. (1980b) Surface evaporation/dissolution partitioning of lower-molecular-weight aromatic hydrocarbons in a down-plume transect from the IXTOC I wellhead. Proceedings: Symposium on Preliminary Results from the September 1979 RESEARCHER/PIERCE IXTOC I Cruise. June 9-10, 1980, Key Biscayne, Florida. pp. 239-263. NTIS Accession Number PB-246068.

Payne, J.R. and G.D. McNabb, Jr. (1984). Weathering of petroleum in the marine environment, *Marine Technology Society Journal* 18(3): 24-42.

Payne, J.R., B.E. Kirstein, G.D. McNabb, Jr., J.L. Lambach, R. Redding, R.E. Jordan, W. Hom, C. de Oliveira, G.S. Smith, D.M. Baxter, and R. Geagel. (1984). Multivariate analysis of petroleum weathering in the marine environment - subarctic. Volume I, Technical Results; Volume II, Appendices. In: Final Reports of Principal Investigators, Vol. 21 and 22. February 1984, U.S. Department of Commerce, National Oceanic and Atmospheric Administration, Ocean Assessment Division, Juneau, Alaska. 690 pp. Volume 21 NTIS Accession Number PB85-215796; Volume 22 NTIS Accession Number PB85-215739.

Payne, J.R., J.R. Clayton, Jr., G.D. McNabb, Jr., and B.E. Kirstein. (1991a). Exxon Valdez oil weathering fate and behavior: Model predictions and field observations. *Proceedings of the 1991 Oil Spill Conference*, American Petroleum Institute, Washington, D.C., pp 641-654

Payne, J.R., L.E. Hachmeister, G.D. McNabb, Jr., H.E. Sharpe, G.S. Smith, and C.A. Manen. (1991b). Brine-induced advection of dissolved aromatic hydrocarbons to arctic bottom waters. *Environ. Sci. Technol.* 25(5): 940-951

Payne, J.R., T.J. Reilly, and D.P. French. (1999). Fabrication of a portable large-volume water sampling system to support oil spill NRDA efforts. *Proceedings of the 1999 Oil Spill Conference*, American Petroleum Institute, Washington, D.C., 1179-1184.

Payne, J.R. and W.B. Driskell. (2001). Source characterization and identification of New Carissa oil in NRDA environmental samples using a combined statistical and fingerprinting approach. *Proceedings, 2001 International Oil Spill Conference,* American Petroleum Institute, Washington, D.C. pp. 1403-1409.

Payne, J.R. and W.B. Driskell. (2003). The importance of distinguishing dissolved- versus oil-droplet phases in assessing the fate, transport, and toxic effects of marine oil pollution. *Proceedings of the 2003 Oil Spill Conference*, American Petroleum Institute, Washington, D.C., pp 771-778.

Payne, J.R., W.B. Driskell, J.F. Braddock, J. Bailey, J.W. Short, L. Ka'aihue, T.H. Kuckertz. (2005). From tankers to tissues – Tracking the degradation and fate of oil discharges in Port Valdez, Alaska. *Proceedings of Arctic Marine Oil Spill Conference 2005*, Calgary, Alberta, Canada. pp 959-991.

Payne, J.R. and W.B. Driskell. (2015a). Forensic fingerprinting methods and classification of DWH offshore water samples. PECI Technical Report to the Trustees in support of the PDARP.

Payne, J.R. and W.B. Driskell. (2015b). Dispersant effects on waterborne oil profiles and behavior. PECI Technical Report to the Trustees in support of the PDARP.

Payne, J.R. and W.B. Driskell. (2015c). Offshore adaptive sampling strategies. PECI Technical Report to the Trustees in support of the PDARP.

Prince, R.C., K.M. McFarlin, J.D. Butler, E.J. Febbo, F.C.Y. Wang, T.J. Nedwed, (2013). The primary biodegradation of dispersed crude oil in the sea, *Chemosphere*, 90(2): 521-526.

Reddy, C.M., J.S. Arey, J.S. Seewald, S.P. Sylva, K.L. Lemkau, R.K. Nelson, C.A. Carmichael, C.P. McIntyre, J. Fenwick, G.T. Ventura, B.A.S. Van Mooy, and R. Camilli. (2011). Composition and fate of gas and oil released to the water column during the Deepwater Horizon oil spill. www.pnas.org/cgi/doi/10.1073/pnas.1101242108. 6 pp.

Redmond, M.C. and D.L. Valentine. (2011) Natural gas and temperature structured a microbial community response to the Deepwater Horizon oil spill. *Proceedings of the National Academy of Sciences*.

Ruddy, B.M., M. Huettel, J.E. Kostka, V.V. Lobodin, B.J. Bythell, A.M. McKenna, C. Aeppli, C.M. Reddy, R.K. Nelson, A.G. Marshall, and R.P. Rodgers. (2014). Targeted Petroleomics: Analytical Investigation of Macondo Well Oil Oxidation Products from Pensacola Beach. *Energy & Fuels* 2014 28 (6), 4043-4050 DOI: 10.1021/ef500427n

Ryerson, T.B., et al. (2011), Atmospheric emissions from the Deepwater Horizon spill constrain air-water partitioning, hydrocarbon fate, and leak rate, *Geophys. Res. Lett.*, 38, L07803, doi:10.1029/2011GL046726.

Ryerson, T.B. R. Camilli, J.D. Kessler, E.B. Kujawinski, C.M. Reddy, D.L. Valentine, E. Atlas, D.R. Blake, J. de Gouw, S. Meinardi, D.D. Parrish, J. Peischl, J.S. Seewald, and C. Warneke. (2012). Chemical data quantify Deepwater Horizon hydrocarbon flow rate and environmental distribution. PNAS 2012 109 (50) 20246-20253.

Smith, R.H., E.M. Johns, G.J. Goni, J. Trinanes, R. Lumpkin, A.M. Wood, C.R. Kelble, S.R. Cummings, J.T. Lamkin, S. Privoznik. (2014). Oceanographic conditions in the Gulf of Mexico in July 2010, during the Deepwater Horizon oil spill, *Continental Shelf Research* 77: 118-131.

Socolofsky SA, Adams EE & Sherwood CR. (2011) Formation dynamics of subsurface hydrocarbon intrusions following the Deepwater Horizon blowout. *Geophys. Res. Lett.* 38: L09602.

Spier, C., W.T. Stringfellow, T.C. Hazen, M. Conrad. (2013). Distribution of hydrocarbons released during the 2010 MC252 oil spill in deep offshore waters. *Environmental Pollution* 173: 224-230.

Stout, S.A. (2015). Review of dispersants used in response to the Deepwater Horizon oil spill. NewFields Technical Report TR02 to the Trustees in support of the PDARP.

White, H.K., S.L. Lyons, S.J. Harrison, D.M. Findley, Y. Liu, and E.B. Kujawinski. (2014). Long-term persistence of dispersants following the Deepwater Horizon oil spill. *Environ. Sci. Technol. Lett.* 1: 295-299.

Wolfe, D.A., M.J. Hameedi, J.A. Galt, G. Watabayashi, J. Short, C. O'Claire, S. Rice, J. Michel, J.R. Payne, J. Braddock, S. Hanna, and D. Sale. (1994). The fate of the oil spilled from the Exxon Valdez. *Environ. Sci. Technol.* 28(13): 561-568

Yapa, P.D., M.R. Wimalaratne, A.L. Dissanayake, J.A. DeGraff Jr. (2012). How does oil and gas behave when released in deepwater?, *J. Hydro-environment Res.* 6(4): 275-285

Appendix 1 – Oil Fate in Advanced Weathering

At the terminus of sampling the deep plume, 412 km from wellhead, analytic results showed no relevant PAH were present (Figure 15). In prior years, it would have been presumed that either microbes had consumed the hydrocarbons or that they had diffused away or settled out as marine snow. Evidence from academic DWH studies using new instruments is suggesting another fate.

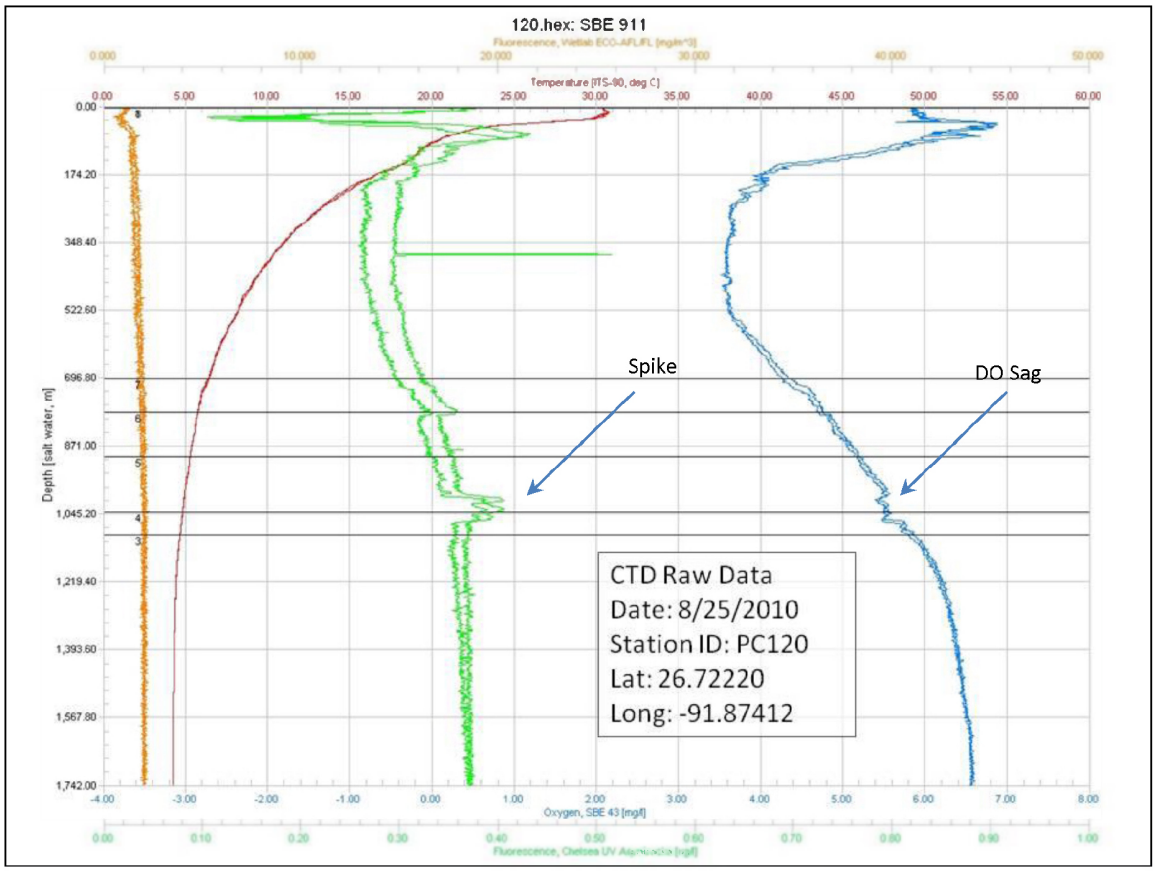

Figure 15. CTD, fluorescence and dissolved oxygen plot showing fluorescence spike (green) and DO sag (blue) at 1038m from *Pisces* cast (412 km from wellhead, bearing 238°). Dispersant indicator, GE, was 23 ng/L; TPAH was 15 ng/L as an inconsequential dissolved signal mostly lost to the lab method blank.

During the last three decades, the combination of GC-FID and GC/MS SIM results has been the gold standard for oil spill forensic work. These instruments and related methods have produced prodigious understanding and insight into oil behavior, and while not yet replaceable as the prime source of reliable data, there have been advancements in instruments introducing new capabilities to analytic oil hydrocarbon chemistry. Adding a second stage of separation, GC x GC/MS, has brought a higher resolution and second dimension of GC/MS components and mass separation in the 8-40 carbon range while providing a facile method of documenting profile changes (Figure 16). Fourier Transformation-Ion Cyclotron Resonance (FT-ICR) mass spectrometry compliments GC/MS abilities by resolving both polar compounds and even heavier masses, in the 20-100 carbon range. Such compounds are often non-chromatographable and far beyond the resolution of GC/MS. Recently, FT-ICR MS, with its ultra-high

resolving power, uniquely identified more than 30,000 acidic, basic, and nonpolar elemental compositions from Deepwater Horizon crude oil (McKenna et al., 2013).

Relevant to our work, FT-ICR analyses have confirmed that the weathering process in environmental samples (slicks and tar balls) and in laboratory photo-oxidation trials comprises transformations of hydrocarbons to multi-state oxidation (Aeppli et al., 2012, Hall et al., 2013, Ray et al., 2014, Ruddy et al. 2014). Ray et al., report that photo-oxidation is a UV driven process that initially adds a single oxygen to oil and increases the water-soluble fraction. The resulting oxidized hydrocarbons are then prone to adding additional oxygen. Non-irradiated (dark) samples were predominantly two-oxygen polar molecules while exposed samples were transformed to predominantly five-oxygen molecules (ranging to eight).

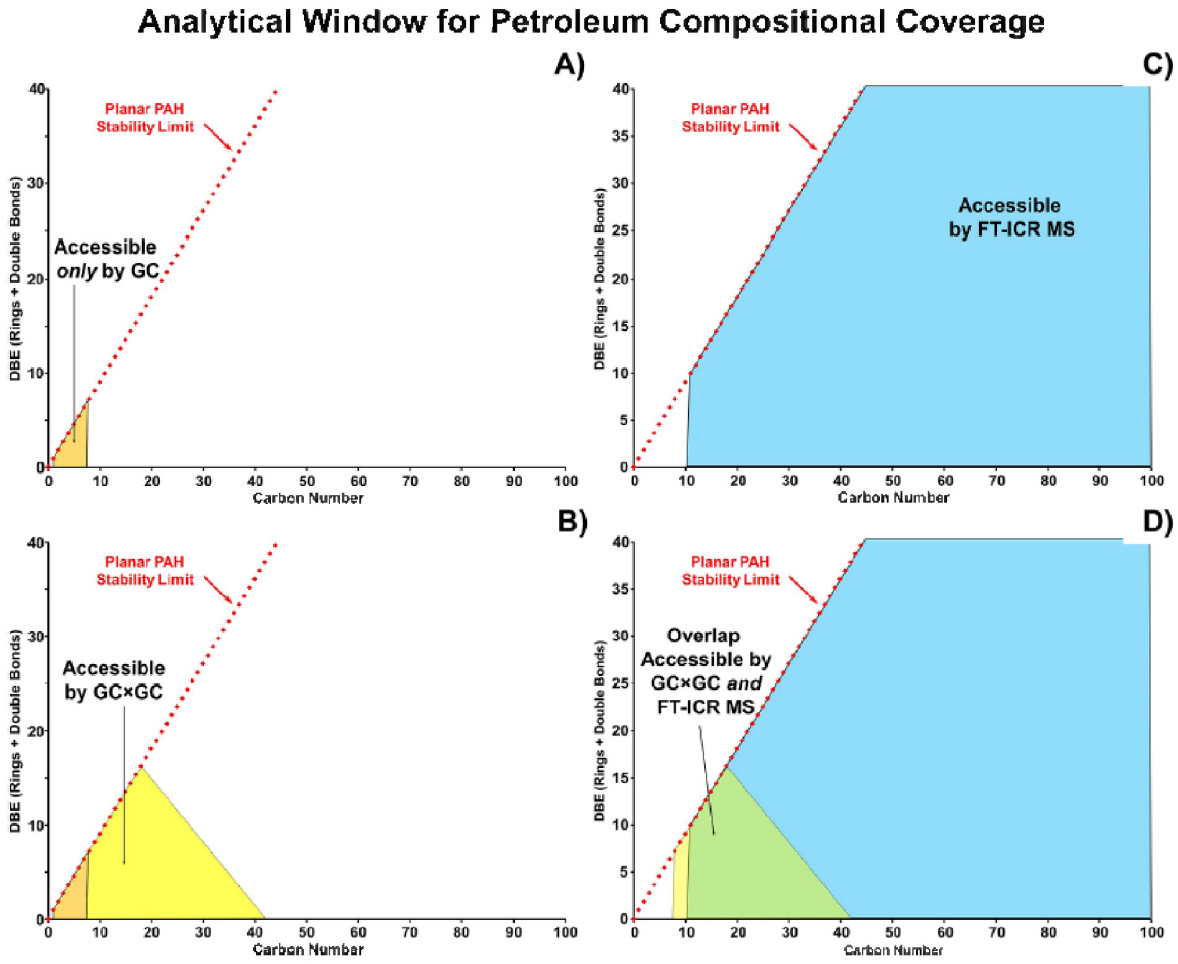

Figure 16. Schematic diagram of the compositional continuum of petroleum (the petroleome) reported as double bond equivalents (DBE, number of rings plus double bonds) versus carbon number. The analytical window accessible only by conventional gas chromatography (GC) is displayed in part A, with the upper boundary limit for all molecules known to exist in petroleum displayed as the PAH planar stability limit. Extension to hybrid analytical techniques (GC × GC) is displayed in Figure B. Part C reports the extension to complete compositional coverage of petroleum molecules (up to C100) that have been observed in Macondo petroleum. Part D combines all three techniques in a single image to highlight

the need for advanced analytical techniques beyond gas chromatography for oil spill science. Figure and caption adapted from McKenna et al., 2013.

Similar processes were seen in DWH slicks and stranded tar ball samples. Aeppli et al., Hall et. al. and Ruddy et al. all report a major shift, predominantly from saturated compounds into oxygenated hydrocarbons (OxHC; Figure 17). Hall suggests the $OxHC_1$ is a transitional state towards $OxHC_2$, a concept reflected in Ray's O_2 to O_5 photo-driven transitions. However, these processes were all the consequence of rigorous surface exposure rather than the dissolution, diffusion and microbial-degradation dominated processes in the dark sub-surface depths.

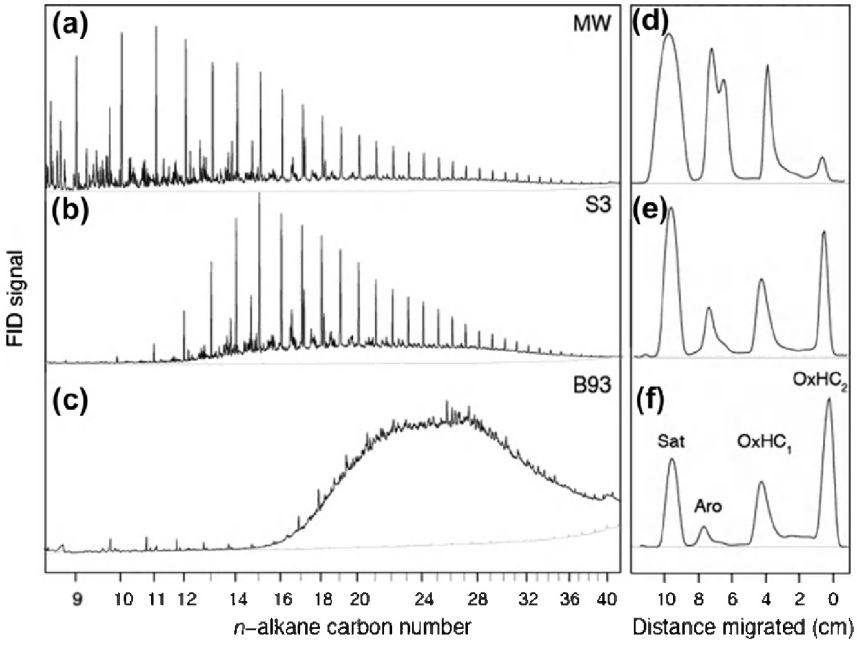

Figure 17. GC-FID traces of (a) Macondo Well (MW) oil (b) surface slick sample S3, and (c) sand patty B93 with corresponding TLC-FID traces (d-f). From GC-FID it can be seen that the sample S3 lost its lighter molecular-weight n-alkanes and one- and two-ring aromatics relative to MW. The more weathered sand patty sample B93 even lost all its n-alkanes, due to the weathering processes like evaporation, biodegradation, and photo-oxidation. As a result, non-GC amenable oxygenated compounds are formed, as can be seen from TLC-FID (Sat = saturated, Aro = aromatic, OxHC = oxygenated hydrocarbon fractions 1 and 2). Figure and caption adapted from Hall, et al. 2013.

There has been a wealth of DWH microbial studies documenting the appearance and hydrocarbon-degrading capabilities of microbial blooms and successional community shifts within and outside the deepwater oil plume in response to available hydrocarbon resources (reviewed in Kimes et. al, 2014). Most studies identify the microbes and their genomically-implied, hydrocarbon-degrading capabilities, but Gutierrez et al. (2013) actually measured hydrocarbon degradation by dominant species using stable isotope probes. The pathways of microbial degradation are well known, driven primarily by monooxygenase and dioxygenase enzymatic reactions that add one or two oxygens to the molecule, forming alcohols, ketones or carboxylic acids (Kimes et al. 2014, Prince and Walters, 2007). The alkanes and cycloalkanes make up the bulk of initially transformed hydrocarbons although simultaneously other microbes are beginning to blossom and catabolize other compound groups respective of their enzymatic capabilities. Ziervogel and Arnosti (in press) expand the concept by suggesting the microbial communities involved in oil degradation include a cascade of primary oil degraders *and secondary*

consumers, which metabolize oil degradation products as well as other bacterial metabolites of primary oil degraders (Head et al., 2006). They further add that a major fraction of oil degradation products typically include protein- and carbohydrate-rich organic molecules (Hazen et al., 2010) while metabolites include bacterial exopolymeric substances (EPS) that are produced in large amounts by oil degraders to emulsify the crude oil (Hino et al., 1997).

The point is that aerobic microbial degradation at depth is well documented and the dominant pathways known. The transformation end products are oxygenated hydrocarbons that are then processed further by various internal metabolic pathways. While deep-plume water samples such as those in Figure 15 have not yet been analyzed by methods capable of resolving the polar components, the obvious expectation is that results would show oxygenated hydrocarbons becoming more prevalent as the oil constituents are degraded, i.e., become more polar and less resolvable by GC/MS. We interpret the fluorescent spike and DO sag still present 412 km from the wellhead with no relevant PAH to represent the oxidized microbial-degraded hydrocarbons non-amenable to GC/MS detection.

Appendix References

Aeppli, C., C.A. Carmichael, R.K. Nelson, K.L, Lemkau, W.M. Graham, M.C. Redmond, D.L. Valentine, and C.M. Reddy. (2012). Oil weathering after the Deepwater Horizon disaster led to the formation of oxygenated residues. *Environ. Sci. Technol.* 46: 8799-8807.

Gutierrez, T., D.R. Singleton, D. Berry, T. Yang, M.D. Aitken, and A. Teske. 2013. Hydrocarbon-degrading bacteria enriched by the Deepwater Horizon oil spill identified by cultivation and DNA-SIP. *ISME J.* 7, 2091–2104. doi: 10.1038/ismej.2013.98

Hall, Gregory J., Glenn S. Frysinger, Christoph Aeppli, Catherine A. Carmichael, Jonas Gros, Karin L. Lemkau, Robert K. Nelson, Christopher M. Reddy. 2013. Oxygenated weathering products of Deepwater Horizon oil come from surprising precursors. *Mar. Pollut. Bull.* 75: 140–149. dx.doi.org/10.1016/j.marpolbul.2013.07.048

Hazen, Terry C., Eric A. Dubinsky, Todd Z. DeSantis, Gary L. Andersen, Yvette M. Piceno, Navjeet Singh, Janet K. Jansson, Alexander Probst, Sharon E. Borglin, Julian L. Fortney, William T. Stringfellow, Markus Bill, Mark E. Conrad, Lauren M. Tom, Krystle L. Chavarria, Thana R. Alusi, Regina Lamendella, Dominique C. Joyner, Chelsea Spier, Jacob Baelum, Manfred Auer, Marcin L. Zemla, Romy Chakraborty, Eric L. Sonnenthal, Patrik D'haeseleer, Hoi-Ying N. Holman, Shariff Osman, Zhenmei Lu, Joy D. Van Nostrand, Ye Deng, Jizhong Zhou, Olivia U. Mason. (2010) Deep-sea oil plume enriches indigenous oil-degrading bacteria. *Science* 330: 204-208.

Head, I.M., D.M. Jones, W.F.M. Röling, 2006. Marine microorganisms make a meal of oil. *Nature Rev. Microbiol.* 4,173–182.

Hino, S., K. Watanabe, N. Tatkahashi, 1997. Isolation and characterization of slime- producing bacteria capable of utilizing petroleum hydrocarbons as a sole carbon source. *J.Ferment.Bioeng.* 84:,528–531.

Kimes, Nikole E., Amy V. Callaghan, Joseph M. Suflita and PamelaJ.Morris. 2014. Microbial transformation of the Deepwater Horizon oil spill—past, present, and future perspectives. *Front. Microbiol.* 5:603. doi:10.3389/fmicb.2014.00603

Ray, Phoebe Z., Huan Chen, David C. Podgorski, Amy M. McKenna, Matthew A. Tarr. 2014. Sunlight creates oxygenated species in water-soluble fractions of Deepwater Horizon oil. *J. HazMat* 280: 636–643.

Ruddy, Brian M., Markus Huettel, Joel E. Kostka, Vladislav V. Lobodin, Benjamin J. Bythell, Amy M. McKenna, Christoph Aeppli, Christopher M. Reddy, Robert K. Nelson, Alan G. Marshall, and Ryan P. Rodgers 2014. Targeted Petroleomics: Analytical Investigation of Macondo Well Oil Oxidation Products from Pensacola Beach. *Energy & Fuels* 2014 28 (6), 4043-4050 DOI: 10.1021/ef500427n

McKenna, A.M., R.K. Nelson, C.M. Reddy, J.J. Savory, N.K. Kaiser, J.E. Fitzsimmons, A.G. Marshall, and R.P. Rodgers. (2013). Expansion of the analytical window for oil spill characterization by ultrahigh resolution mass spectrometry: Beyond gas chromatography. *Environ. Sci. Technol.* 47: 7530-7539.

Prince R., C. Walters, 2007. Biodegradation of oil hydrocarbons and its implications for source identification. In Oil Spill Environmental Forensics. Wang Z, Stout S. eds. Academic Press. 2007:349–379.

Ziervogel, Kai, Carol Arnosti. In press. Enhanced protein and carbohydrate hydrolyses in plume-associated deep waters initially sampled during the early stages of the Deepwater Horizon oil spill. *Deep-SeaRes.II* (2013), http://dx.doi.org/10.1016/j.dsr2.2013.09.003i